ABSTRACT

Title of Document: ALTERNATIVE SUBSTRATES FOR RESTORATION OF THE CHESAPEAKE BAY'S EASTERN OYSTER, *CRASSOSTREA VIRGINICA*: AN EVALUATION USING ADDITIVE MANUFACTURING AND ELECTROLYSIS MINERAL ACCRETION

Myles Arrington, Aaron Auerbach, Nellie Gold-Pastor, Nathan Mengers, Cara Schiksnis, Caroline Simon

Directed by: Dr. Kennedy Paynter, Marine-Estuarine Environmental Sciences

Over the past century, the population of the Chesapeake Bay's eastern oyster, *Crassostrea virginica,* has collapsed dramatically, endangering the ecology of the bay and economy of the surrounding area. Declining shell numbers limit the growth of current oyster populations and have led to the use of alternative substrate material as a method for oyster restoration. Motivated by successful coral reef restoration efforts and the emerging field of additive manufacturing, we tested the use of electrolysis mineral accretion and Fused Deposition Modeling (FDM) to create artificial substrate for oyster spat settlement and survival. To start, we employed electrolysis mineral accretion with the goal of creating a sustainable and adequate amount of calcium carbonate ($CaCO_3$) substrate. Mineral accretion rates were restrictive in our closed system, and we were unable to create sufficient substrate to test settlement. Second, we used 3D scanning and FDM to print artificial oyster shells identical to their natural counterparts, using a filament containing $CaCO_3$. Using 3D printed oyster shells, we tested the importance of physical structure versus the presence of intrinsic biochemical cues in oyster settlement rates. Our results indicated that the oyster spat did not achieve significant survival on the printed material. Similarly, the use of the

biochemical cue L-DOPA was insufficient in encouraging larval settlement on printed shells, indicating the significant role played by the underlying shell composition. The results indicate that the biochemical properties of the substrate take precedence over the geometric similarity to natural shells, a finding which should guide future methodology in oyster restoration.

ALTERNATIVE SUBSTRATE FOR RESTORATION OF THE CHESAPEAKE BAY'S EASTERN OYSTER, *CRASSOSTREA VIRGINICA*: AN EVALUATION USING ADDITIVE MANUFACTURING AND ELECTROLYSIS MINERAL ACCRETION

By

Team Oysters

Myles Arrington
Aaron Auerbach
Nellie Gold-Pastor
Nathan Mengers
Cara Schiksnis
Caroline Simon

Thesis submitted in partial fulfillment of the requirements of the Gemstone Program
University of Maryland, College Park
2019

Advisory Committee:
Dr. Kennedy Paynter, Mentor
Ms. Audrey McDowell, Discussant
Ms. Marybeth Shea, Discussant
Mr. Preston Tobery, Discussant
Dr. Lance Yonkos, Discussant

Acknowledgements

We would like to express our sincere appreciation to our advisor, Dr. Kennedy Paynter, for his constant support, knowledge, and enthusiasm for our project. We are grateful for the assistance of the Paynter Lab, Drew Needham, Sandra Davis, and Audrey McDowell. We also wish to thank the VIMS Eastern Shore Laboratory and the Horn Point Oyster Hatchery, especially Stephanie Alexander for her help with data collection. We appreciate the guidance and hard work of Preston Tobery with our 3D printing endeavours. We are also thankful for the access we have as students to 3D printing technology at the John and Stella Graves Makerspace and Terrapin Works. We also wish to thank our librarian, Stephanie Ritchie. We would like to thank the incredible Gemstone faculty and staff including Dr. Frank Coale, Dr. Kristan Skendall, Vickie Hill, Leah Tobin, and Jessica Lee for a remarkable four years. Also, thank you to our four discussants for reviewing our thesis and offering their well-informed recommendations. Finally, we are indebted to our loving families for their support throughout our undergraduate careers.

Table of Contents

List of Figures

List of Tables

General Introduction

Planet Earth has sustained life for millions and millions of years, giving way to increasing complexity, diversity, and beauty in its ecosystems over that time. However, this longevity and self-sustainability may not last much longer. Recent research indicates that not only are individual ecosystems and biosystems at risk of environmental collapse, but that there are also global-level threats to Earth's sustainability. As a result, scientists, researchers, and policy-makers have invested in addressing this issue, proposing creative solutions that would ensure efficient use of resources, enable the use of alternative resources, and provide for the future of the next generation. Many of these solutions start on a relatively smaller scale with a focus on a particular ecosystem or population. The end goal is to have a lasting effect in that region. In theory, these efforts would contribute to the larger goal of addressing the overall sustainability of the planet.

Following this focused approach, this paper details recent efforts by researchers to contribute to improving the health of a local ecosystem, the Chesapeake Bay. The bay is important to the ecosystem of not only the state of Maryland, but also the Atlantic coast, and has been of primary concern to researchers and ecologists in recent years. The authors are a six-member undergraduate research team called Team Oysters, which is mentored by Dr. Kennedy Paynter and is a part of the Gemstone Honors Program at the University of Maryland, College Park. In 2016, the team began by exploring the process of electrolysis mineral accretion as method for creating alternative substrate for oyster habitat. In Fall 2017, the pre-existing teams Oysters and WALK combined, giving way to the current team composition along with a new direction in the project that incorporates additive manufacturing, specifically 3D

printing. Though the methodology has changed over the years, the team has maintained the goal of seeking innovative, creative, and adaptive ways to do study alternative oyster reef habitat in the Chesapeake Bay. The following paper is split into three different sections, detailing the team's research over the three-year time period. The first portion is a general literature review for the project, describing *C. virginica* biology and restoration efforts. In this portion, we also discuss our goals and questions that guide the direction of our project. The second portion of the paper discusses the beginning of the project, including research into the use of electrolysis mineral accretion towards restoration efforts. Lastly, the final section details the second part of the project, including the use of 3D printing in restoration research, and two separate phases of settlement testing.

This research represents a novel method for examining substrate availability for *C. virginica*, and proposes insight into the direction of future oyster restoration research. Given the critical role that the oyster plays in the Chesapeake Bay's ecosystem, this research could be crucial in improving the sustainability of the bay and its inhabitants at large, making it a viable stepping stone for continued research.

A Review of Literature on the Eastern Oyster

Keystone Species

Scientists know that a small subset of species can have a disproportionately large effect on ecosystems, even if they represent a minute portion of the population or biomass (Müller, Bußler, Goßner, Rettelbach, & Duelli, 2008). Known as a keystone species, this organism is linked to the function and survival of a wide array of species, and plays a critical role in the organization and function of their surrounding ecosystem (Müller et al., 2008). The eastern oyster, *Crassotrea virginica*, native to the Chesapeake Bay, is a keystone species due to its role as a biofilter, a hard substrate for other organisms to utilize as shelter and habitat, and prey for numerous predators, all of which are integral to the health and survival of other species within the Chesapeake Bay's estuarine ecosystem (O'Connell, Franze, Spalding, & Poirrier, 2005).

Background

The eastern oyster is a stationary bivalve mollusk in the Ostreidae family that has adapted to deep-water and estuarine habitats (Allen et al., 2014). This oyster can survive in both brackish water with low salt levels and hypersaline water with high salt levels (Allen et al., 2014). The range of the eastern oyster extends along the eastern coast of North America from the Gulf of St. Lawrence to the Gulf of Mexico (Allen et al., 2014). The eastern oyster has numerous behavioral adaptations that allow it to tolerate wide variations in temperature, salinity, suspended sediments, and dissolved oxygen (Allen et al., 2014). Despite the resiliency of the eastern oyster, a reduction in available substrate for oyster settlement has put this oyster population at risk (Waldbusser, Voigt, Bergschneider, Green, & Newell, 2011). Other risks include disease, sedimentation, overharvesting, and eutrophication, which have led to the

decline of the eastern oyster population to historically low levels, threatening the overall health of the Chesapeake Bay. (Waldbusser et al., 2011). Overall, the ecological vitality of the Chesapeake Bay depends in part on the eastern oyster due to its significant role as a keystone species.

Life Cycle

Under ideal conditions, eastern oysters can live up to forty years and grow up to eight inches long (Allen et al., 2014). During the summer and autumn months, adult oysters release eggs and sperm into the water, where external fertilization then occurs (Allen et al., 2014). The females are able to spawn more than once a season and one female is capable of releasing up to twenty million eggs (Allen et al., 2014). Oyster larvae are meroplanktonic, and are carried through the water by currents during their early stages of life, about two to three weeks after fertilization (Allen et al., 2014; Sellers & Stanley, 1984). During this phase, the oyster larvae go through several stages of development; the blastula, gastrula, the trochophore, prodissoconch I and II, in which the larvae develop a straight-hinge shell and a ring of locomotory cilia (called the velum), and later pronounced umbones (Sellers & Stanley, 1984). At the end of the larval developmental period, larvae grow an elongated foot with a large byssal gland and tend to sink to the ocean floor to look for substrate suitable for settlement (Allen et al., 2014; Sellers & Stanley, 1984).

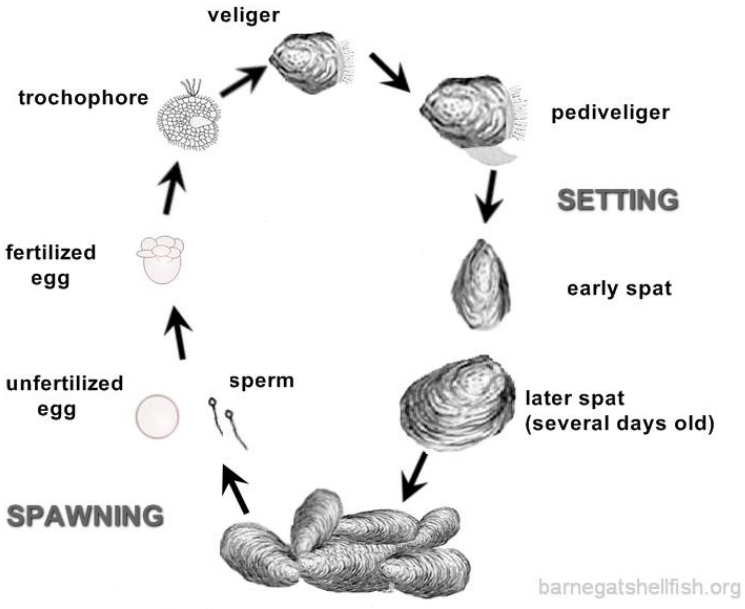

Figure 1: Diagram of eastern oyster life cycle (Barnegat Bay Shellfish)

Approximately two to three weeks after spawning occurs, oyster larvae enter the juvenile stage, at which point they begin to seek solid surface in preparation for metamorphosis (Sellers & Stanley, 1984). During this time period, the juvenile oysters 'crawl' using this protruding foot gland to seek appropriate substrate for settlement (Sellers & Stanley, 1984). Larval settlement typically requires hard substrate, which is usually composed of the calcium carbonate shells of living and dead oysters (George, De Santiago, Palmer, & Beseres Pollack, 2015; Waldbusser et al., 2011). If suitable substrate is not found, the larvae are not able to settle and will not survive (Allen et al., 2014). Although oysters are capable of producing millions of spat, it is the amount of substrate available that largely determines the next generation's population size (Allen et al., 2014).

Oyster larvae settlement behavior is induced by environmental cues including increased water temperature, changes in salinity, changes in phytoplankton biomass, and other biochemical cues that are characteristically associated with the preferred substrate for settlement (Coon et al., 1985; Horn Point Lab Oyster Hatchery; Sellers

& Stanley, 1984). It has been suggested that these environmental cues initiate metamorphosis through the stimulation of neural and or hormonal processes (Burke, 1983). Eastern oyster larvae have been shown to have preferential settlement behavior on existing oyster reefs (Burke, 1983; Sellers & Stanley, 1984).

Under ideal environmental conditions and once appropriate substrate is found, juvenile larvae undergo metamorphosis into a sessile organism (Baker & Mann, 1994). As the oyster transitions into the spat stage, the foot attaches to the substrate and the oyster begins growing its shell (Nayer et. al, 1984; Sellers & Stanley, 1984). Oyster shells are vital for oyster survival; they support the oyster tissue, protect from predators, and defend against mud and silt (Waldbusser et al., 2011). These shells are formed from calcium carbonate sequestered from the water column; this process begins with the formation of a periostracum, the outer layer of the shell in the mantle folds (Horn Point Lab Oyster Hatchery; Waldbusser et al., 2011). This is followed by the deposition of an organic matrix and flow of calcium carbonate within it (Waldbusser et al., 2011). The rate at which oysters undergo metamorphosis varies considerably, occurring at times in less than twenty-four hours or up to several days between stages (Baker & Mann, 1994). On average oysters that completed metamorphosis successfully do so within the first 1-3 days post-settlement (Baker & Mann, 1994; Sellers & Stanley, 1984). Oysters typically grow up to one inch per year depending on water conditions, and reach adulthood at about three years (Horn Point Lab Oyster Hatchery).

Oyster Reefs

Oyster reefs play an important ecological role in the estuarine ecosystem because they provide a desirable habitat for other marine organisms (Piazza, Piehler, Gossman, La Peyre, & La Peyre, 2009; Waldbusser et al., 2011). Playing a similar

role to coral reefs in oceanic environments, the oyster reef provides habitat and food for benthic organisms, commensal macrofauna, invertebrates and fish in the estuarine environment (Tolley & Volety, 2005). Organisms such as barnacles, mussels, and anemones use substrate created from oyster reefs to attach and grow, while mollusks, worms, fish, and crabs use the reef shape as shelter and spawning areas (Horn Point Lab Oyster Hatchery). Reefs are typically found in shallow, tidal waters where oysters settle to make expansive colonies (Styles, 2015). Many reefs cluster near winding curves or areas of confluence between rivers in regions favorable to an eddy formation (Styles, 2015). The location of an oyster reef along shorelines plays a significant role in the anchorage of sediments and helps stabilize channel banks vulnerable to erosion (Styles, 2015). Coastal protection efforts benefit from the structural support of oyster reefs as they protects coastal habitat and development from tropical storms (Piazza et al., 2009).

In the last 130 years, about 85% of oyster reefs have been lost globally, raising concerns about the viability of future oyster populations and other related marine species, which depend on existing oyster reefs for settlement and habitat (O'Connell et al., 2005; Grabowski et al., 2012). The decline in oyster populations throughout the world can be attributed to several factors, including ocean acidification, which affects all marine organisms worldwide, and specifically in the context of the Chesapeake Bay, eutrophication, sediment pollution, overharvesting, and disease, which have contributed to the decline of the oyster population in the Chesapeake Bay to less than 1% of its historic size (Hargis, & Haven, 1988; Howarth & Marino, 2006; Miller, Reynolds, Sobrino, & Riedel, 2009).

Economic Role of the Oyster

The Chesapeake Bay's commercial fishing industry relies heavily on the eastern oyster population (Kasperski & Wieland, 2009). Overall, the commercial eastern oyster fishery in Maryland and Virginia contributed $51 million in sales in 2015, according to that year's Fisheries Economics of the U.S. report by the National Oceanic and Atmospheric Administration (National Marine Fisheries Service, 2017). The commercial fishery industry of the Chesapeake Bay continues to be threatened by the continuous decline of the eastern oyster population (Kasperski & Wieland, 2009). Over the past 30 years, Mayland and Virginia have suffered $4 billion in losses due to the decline in the bay's oyster population.

The economic role of the oyster population is not limited to the markets that surround them. As a keystone species, oyster survival determines the health of other marine organisms and its surrounding environment. Acting as a biofilter, the oyster population of the Choptank River is estimated to have prevented costs of over $300,000 a year through nitrogen pollution removal, which would otherwise be done by wastewater treatment systems (Beseres Pollack, Yoskowitz, Kim, & Montagna, 2013). In a paper published in 2012 in *Bioscience*, Grabowski et al. estimated the total value of oysters in terms of services provided through habitat for other marine organisms, contributions to water quality and health, erosion protection, and other services adding up to an annual value ranging between $10,325 to $99,421 per hectare of oyster reef depending on location (Grabowski et al., 2012). The following figure is a summary of their findings:

Ecosystem service values	Minimum	Maximum	Average
Oyster habitat state			
Pristine	12,186	21,959	17,072
Degraded	880	880	880
Finfish and mobile crustacean value			
Recreational	n/a	n/a	n/a
Commercial	4123	4123	4123
Water quality services			
Chlorophyll *a* removal[a]	0	0	0
Nitrogen removal[b]	1385	6716	4050
Recreational use	n/a	n/a	n/a
SAV enhancement[c]	0	2584	1292
Bacterial removal	n/a	n/a	n/a
Carbon burial	n/a	n/a	n/a
Shoreline protection[c]	0	85,998	860
Habitat for epibenthic infauna	0	0	0
Landscape processes	0	0	0
Nonoyster harvest service total	5508	99,421	10,325

Note: n/a represents insufficient data to assess the economic value of the service.
[a]The value of chlorophyll *a* removal was not included in the summary table because this service is considered potentially redundant if nitrogen removal through denitrification is also considered.
[b]The value of nitrogen removal was estimated by quantifying the value of enhanced denitrification rates on oyster reefs.
[c]The average submerged aquatic vegetation (SAV) enhancement and shoreline stabilization was valued assuming that 1% of the linear length of reefs perform this function.

Figure 2: Total annual value of ecosystem services provided by oyster reefs in 2011 dollars per hectare per year. Source: (Grabowski et al., 2012).

To combat the decline in the oyster population and support the economic vitality of the bay, scientists are developing oyster aquaculture to alleviate harvesting stresses on the wild eastern oyster population (Williamson, Tilley, & Campbell, 2015). Disease-resistant aquaculture could increase oyster stock for commercial fisheries (Williamson et al., 2015). Aquaculture must overcome strict regulatory policies in order to flourish and have a positive impact on the health of the Chesapeake Bay and its economy (Hopkins et al., 1995). Fishery management policy has led to bottom-lease accessibility for aquaculturists and an increase in triploid

oyster stock (Maryland Environmental Trust, 2013). Work at the Horn Point Hatchery and Virginia Institute of Marine Science (VIMS) has improved disease resistant triploid oyster stock for aquaculture purchase and had a positive effect on the expansion of the oyster fishery industry (Williamson et al., 2015). Development in oyster aquaculture is predicted to benefit the economy through the creation of new jobs and increase in overall capital (Byron, Jin, & Dalton, 2015).

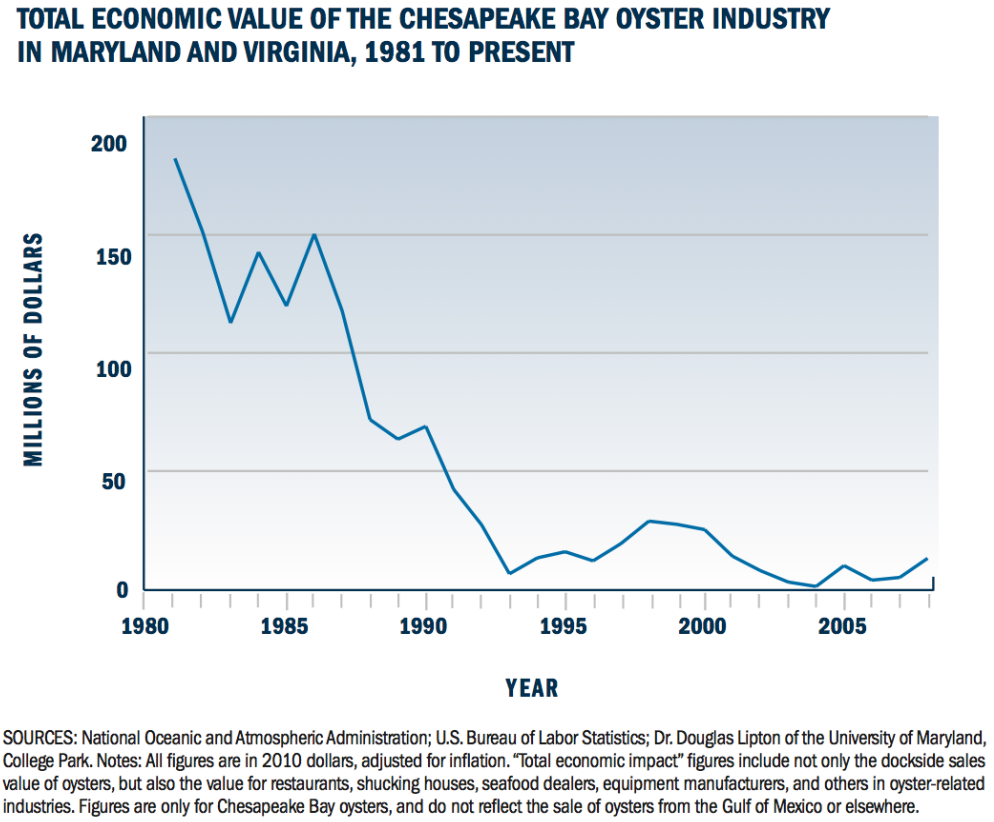

Figure 3: The decline of the economic value of the eastern oyster in the Chesapeake Bay (Goldsborough & Pelton, 2010)

Population Decline Factors

Ocean acidification.

Over the past 200 years, atmospheric carbon dioxide (CO_2) levels have drastically increased, largely due to human activity such as fossil fuel combustion, deforestation, and land development (Doney, Fabry, Feely, & Kleypas, 2009). The

oceans act as a carbon sink, and have captured about one-third of this anthropogenic carbon dioxide from the atmosphere (Miller et al., 2009). The current surplus of atmospheric carbon dioxide has led to ocean acidification, a process that lowers water pH and alters oceanic chemical interactions (Doney et al., 2009; Gazeau et al., 2013).

Carbon dioxide reacts in water to form carbonic acid (H_2CO_3), some of which then dissociates to form a bicarbonate ion (HCO_3^-) and a hydrogen ion (H^+). Some of the bicarbonate ions then lose a hydrogen ion to create carbonate (CO_3^{2-}) As the concentrations of CO_2 increase in the atmosphere, this series of reactions is shifted so that there are more dissolved hydrogen ions in the ocean surface, which react with carbonate to reform bicarbonate, thus reducing the overall amount of carbonate ions in the water and increasing the acidity (Doney et al., 2009). Measurements taken from ocean surface waters since 1760 have demonstrated a decrease in pH of 0.1 units and scientists predict an additional decrease of 0.1 to 0.5 units in the upcoming century (Miller et al., 2009). The reduction of carbonate ions in the system presents an issue for calcifying organisms, such as oysters and coral, which have been found to demonstrate reduced calcification rates, increased mortality rates, decreased growth rates, feeding inhibition, decreased recruitment rates, and abnormal behaviors under ocean acidification conditions (Doney et al., 2009; Gazeau et al., 2013; Waldbusser et al., 2011). Additionally, not only does the decrease in carbonate ions affect adult oysters, but it also poses a risk to oyster larvae seeking hard substrate for settlement, as less calcium carbonate is able to be formed under these conditions (Waldbusser et al., 2011).

According to Doney et al. (2009), the majority of research in this field revolves around the effects of ocean acidification on oceanic ecosystems, with little

attention and focus on estuarine ecosystems such as the Chesapeake Bay (Doney et al., 2009). However, ocean acidification demonstrates a higher risk in estuarine environments; it occurs faster and with more pronounced effects than open ocean waters due to estuaries' lower salinity levels, shallower depths, and lower buffering capacities (Waldbusser et al., 2011).

Eutrophication.

Over the past century, the Chesapeake Bay has experienced a greater inflow of contaminants, specifically pesticides, fertilizers, and other pollutants (Leight, Slacum, Wirth, & Fulton, 2011). Excess nutrients, namely nitrogen and phosphorous, which come largely from sewage treatment plants, septic tanks, and runoff from farms and lawns (Fertig, Carruthers, & Dennison, 2014), lead to eutrophication which causes algal blooms that can create hypoxic or even anoxic conditions within the estuarine waters (National Oceanic and Atmospheric Administration, 2008). Although oysters are known to survive under low oxygen conditions, the disruption of normal processes can be lethal over extensive periods of time (Kennedy, Newell, & Eble, 1996; National Oceanic and Atmospheric Administration, 2008). Similarly, toxic algal blooms such as red tides, brown tides, or *Pfiesteria*, can lead to the release of toxins that have damaging effects on flora and fauna (National Oceanic and Atmospheric Administration, 2008).

Eutrophication occurs due to excess concentrations of both nitrogen and phosphorus; however, nitrogen was identified as the main cause of eutrophication in estuaries, representing the largest threat to the United States's coastal ecosystems (Howarth & Marino, 2006). Nitrogen pollution results from increased use of fertilizer and combustion of fossil fuels (Howarth & Marino, 2006; Talberth, Selman, Walker, & Gray, 2015). Coastal waters nearby agricultural activity and urban centers have the

highest risk of excess nitrogen pollution (Howarth & Marino, 2006). Nutrient concentrations are determined by the ratio of nitrogen to phosphorus, with nitrogen fixation affecting nutrient absorption, and phosphorus regulating primary production (Howarth & Marino, 2006). Phosphates bind to most soils or sediments, and therefore generally enter estuarine waters in surface flows (Correll, 1998).

Overharvesting.

The Chesapeake Bay is also subject to overfishing and overharvesting, causing a decrease in fish and mollusk populations to a reported 1% of their original population size (Rothschild, Ault, Goulletquer, & Heral, 1994). Current unsustainable fishing and dredging methods have had adverse effects on fish and mollusk populations due to the destruction of habitat coupled with increased harvest rates (Rothschild et al., 1994; Wilberg, Livings, Barkman, Morris, & Robinson, 2011). Large-scale commercial fishing began in the Chesapeake Bay in the mid-1800s. By the end of the 19th century, the Chesapeake Bay became the largest commercial fishery in the world, producing 15 million bushels at its peak (Wilberg et al., 2011). Overtime, due to unsustainable fishing practices and population decline from disease and environmental factors, the harvest levels have substantially decreased by 92% (Wilberg et al., 2011).

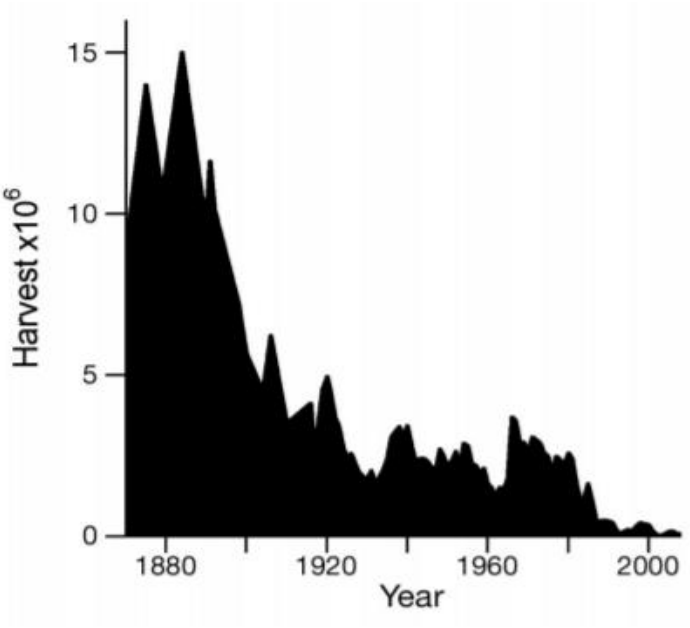

Figure 4: Oyster harvests have declined over the past 150 years (Wilberg et al., 2011)

One example of unsustainable fishing practices in oyster dredging is the usage of hydraulic-powered tongs which break apart oyster reefs and cover them in silt, preventing the future settlement of oyster spat (Rothschild et al., 1994).

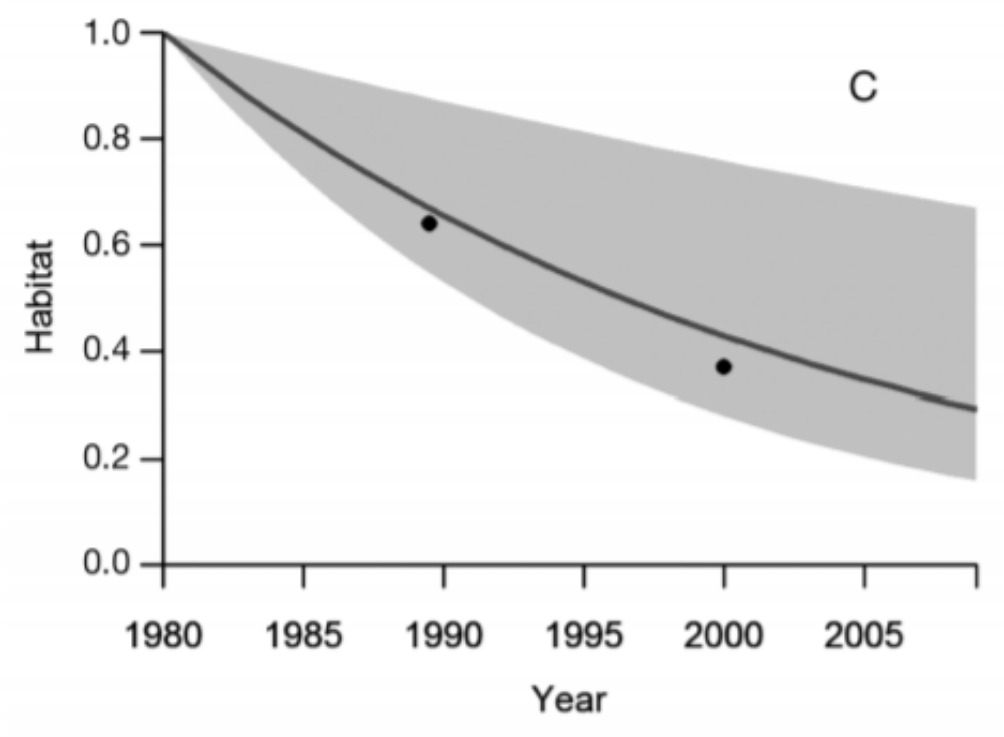

Figure 5: Habitat decline due to overfishing in the Chesapeake Bay (Wilberg et al., 2011)

The Chesapeake Bay is one of the largest and oldest oyster harvesting grounds in which the oyster industry largely depends on wild oyster harvests (Goldsborough & Pelton, 2010). As stated in a 2009 study by the Maryland Oyster Advisory Commission, experts listed illegal oyster harvesting activities as one of the most important challenges facing oyster restoration efforts and aquaculture, as many oyster fishermen are resistant to controls on land that had historically been open for all to harvest (Goldsborough & Pelton, 2010). Poaching represents an extension of overharvesting, despite legislative and policy attempts to provide sanctuary space for restoration efforts to take place.

Disease.

The diseases Dermo and Multinucleated Sphere Unknown (MSX) have greatly contributed to the overall decline of the oyster population in the Chesapeake Bay (Paynter & Burreson, 1991). MSX occurs as a result of the parasitic protozoan, *Haplosporidium nelsoni*, while the protozoan known as *Perkinsus marinus* causes Dermo (Paynter & Burreson, 1991). MSX and Dermo are capable of killing as much as 50-90% of affected oysters (Yu & Guo, 2006). Although certain species of oysters have evolved over time or have been bred to be disease-resistant, the population in the Chesapeake Bay has shown no evidence of disease resistance to MSX or Dermo (Paynter & Burreson, 1991).

Dermo infections can occur in hypersaline waters (greater than 15 parts per thousand (ppt)) and in salinities less than 10 ppt (Paynter, 1996). The main symptom of the infection is a reduction or halt in oyster growth rate and a high mortality rate, typically associated with high water temperature in the summer from August to September (Paynter, 1996). The disease progresses from time of infection with the disease affecting several cell-mediated responses such as ciliary beating, respiration

and absorption of food, to the eventual death of the oyster. Little is known about the cause of death (Paynter, 1996).

Unlike the Dermo disease, MSX infections occur predominantly in hypersaline waters (Horn Point Lab Oyster Hatchery). The infection is known to significantly affect oyster reproduction by inhibiting gametogenesis and causing disruptions in carbohydrate metabolism, thereby reducing fertility rates (Paynter, 1996). MSX is known to result in the quick death of oyster spat (Horn Point Lab Oyster Hatchery). Both diseases combined with the overharvesting of oysters have been identified as major causes of the declining oyster population in the Chesapeake Bay (Paynter & Burreson, 1991).

Sediment pollution.

Heavy rainfall and natural disasters cause changes to the estuarine waters such as lower salinity and increased concentration of suspended sediments, which can have inimical effects on the health of oysters (Hargis & Haven, 1988). For example, tropical storm Agnes of June 1972 reported oyster population losses of up to 70% in the Potomac River tributaries of the Chesapeake Bay (Wilber & Clarke, 2001; Hargis, & Haven, 1988). Stormwater pollution, whether it occurs by natural disasters or heavy rainfall, carries litter, nutrient waste, animal waste, dead foliage, and sediment pollution from surrounding areas (Office of Environment & Heritage, 2013). Sediment pollution includes soil erosion, runoff of substrate from building sites, and displacement of underwater sediment (Office of Environment & Heritage, 2013).

There are multiple risks of sediment pollution such as decreased depth of the photic zone, changes to stratification in the water column, and deterioration of water quality (Kerr, 1995; Wilber & Clarke, 2001). Larval development rates can slow due to sedimentation, which increases predation and reduces survival rates (Wilber &

Clarke, 2001). When suspended sediment concentrations surpass the threshold at which bivalves can efficiently filter material, adult bivalves will reduce their net pumping rates and reject excess material as waste (Wilber & Clarke, 2001). Similarly, in juvenile oysters, high concentrations of suspended materials diminish their ability to ingest algae (Wilber & Clarke, 2001). In both cases, over-sedimentation reduces the availability of food resources, suppresses ingestion, and therefore can interfere with growth and survival rates (Wilber & Clarke, 2001). Further, sediment in the bay settles at the bottom and covers up the hard surfaces necessary for oyster settlement, thus reducing substrate availability for oysters (Kennedy, 1996).

Restoration Efforts

Alternative substrate research.

Past and present oyster restoration efforts in the Chesapeake Bay generally focus on the placement of alternate substrate on the seafloor to serve as a site for oyster recruitment and growth (Nestlerode, Luckenbach, & O'Beirn, 2007). Ideally, these alternate substrates become covered overtime with a layer of oyster shells, producing an oyster reef. Naturally, oyster larvae prefer to settle on living or recently living shells of conspecifics (Nestlerode et al., 2007; Kennedy et al., 1996). Larval settlement preferences are related to the presence of pheromones and survival success (Kennedy et al., 1996). The most desirable substrate for artificial oyster reef construction is empty, shucked eastern oyster shells that have been collected from food operations or historic deposits of oyster shell reefs (Kennedy et al., 1996). When old or dead shells are compiled into mounds, an interstitial matrix of space between shell fragments is produced (Nestlerode et al., 2007). An interstitial matrix provides desirable settlement habitat for oysters and other reef dwelling organisms (Nestlerode et al., 2007). Since the 1990s, restoration efforts in the Chesapeake Bay have been

centered on the introduction of reefs built as three-dimensional mounds, mostly for placement in the intertidal zone (Nestlerode et al., 2007). However, oyster restoration efforts have been forced to look to alternate substrates for reef construction in order to address the problem of oyster population decline. Materials such as granite, concrete, limestone marl, pelletized coal ash, and steel slag as well as the shells of other benthic organisms including surf clamshell or fossil shells from surface mines can serve as suitable alternate substrates (U.S. Army Corps of Engineers, 2012; Nestlerode et al., 2007; Schuhmacher & Schillak, 1994).

Currently, there are multiple programs for oyster restoration in the Chesapeake Bay (National Oceanic and Atmospheric Administration, 2015). One notable program is the Chesapeake Bay Oyster Recovery by the U.S. Army Corps of Engineers. The project focuses on oyster restoration using multiple substrates including oyster shell, clam shell, crushed concrete, rock, and reef balls (National Oceanic and Atmospheric Administration, 2015). While cement, granite and other similar substrates have had successful results, they pose higher risks to the environment due to their toxicity and environmental integration methods (U.S. Army Corps of Engineers, 2012). Artificial reefs traditionally take many years before they are integrated into the marine ecology for reef organisms to settle or grow upon them (U.S. Army Corps of Engineers, 2012). Generally, these structures resist environmental integration due to toxic chemicals or trace metals that seep from the substrates used to create the artificial reef for many years after their placement, slowing down the timeline for reef restoration (Hilbertz, 1981).

While surf clam and other shells are natural alternatives to artificial substrates, their supply declines alongside the eastern oyster population (U.S. Army Corps of Engineers, 2012). The use of fossil shells from surface mines or purchase of natural

shells from other states, such as Florida, has disadvantages such as unknown reserves and potential damage to the natural environment (U.S. Army Corps of Engineers, 2012). While the utilization of naturally occurring shells is generally most successful in achieving viable restoration reefs, the declining supply of this resource indicates that the usage of naturally occurring shells is not a sustainable mechanism for restoration in the future.

Oyster sanctuaries and reserves.

An additional ongoing method of oyster restoration in the Chesapeake Bay is the creation and maintenance of oyster sanctuaries and oyster reserves. A sanctuary is an area in which the harvest of oysters is prohibited by the law (NCDEQ, n.d.). Within these designated areas, restoration researchers implement materials such as recycled oyster shells, Reef Balls, and crushed concrete on which oyster spat have usually already been planted in order to create a successful population in the protected area (NCDEQ, n.d.). In 2009 and 2010, Maryland's Oyster Restoration and Aquaculture Development Plan expanded oyster sanctuaries in the Chesapeake Bay and surrounding river system from 9% to 25%, bringing the amount of protected space up to 9,000 acres (Maryland Department of Natural Resources). The major goals of this plan were to restore oyster broodstock to the Chesapeake Bay by lowering disease, protect oysters from harvesting and poaching activities, and provide the ecological functions of a healthy oyster bar (Maryland Department of Natural Resources).

According to the 2016 Oyster Management Review conducted by the Maryland Department of Natural Resources on the sanctuaries established in Maryland in 2009 or 2010, survival of oysters remained the same or increased since the sanctuary creations (Maryland Department of Natural Resources, 2016). This

same outcome was measured to have occurred in sanctuaries established before 2009 and 2010, with the exception of three sanctuary areas that were established in periods of high disease mortality (Maryland Department of Natural Resources, 2016). In addition to increased survival, biomass in sanctuaries also increased, achieving the highest recorded biomass levels within the past 26 years of the Chesapeake Bay, although majority of this increase was attributed to low salinity areas (Maryland Department of Natural Resources, 2016).

Figure 6: Retrieved from Maryland Department of Natural Resources, 2016 Monitoring Report. Average oyster biomass index calculated for oyster sanctuary areas in Maryland utilizing Fall Survey data 1990 - 2015 pooled from over 12 sanctuary areas

Unlike sanctuaries, oyster reserves allow for the harvest of oysters, but under controlled conditions (Maryland Department of Natural Resources). Periodically, the Maryland Department of Natural Resources (DNR) closes these areas to harvesting activities and re-seeds the area with spat using substrate methods similar to those used for sanctuaries (Maryland Department of Natural Resources). After being restored with a healthy and sizeable local oyster population, the department reopens the

reserve for harvest (Maryland Department of Natural Resources). Watermen who harvest within the reserve are responsible for returning their shucked oyster shells to the reserve, which are collected and used in the next larvae re-seeding event (Maryland Department of Natural Resources). Maryland currently has 12 oyster reserves, though funding and resources such as recycled oyster shell are becoming increasingly less available (Maryland Department of Natural Resources).

Team Oysters Goals

To improve on current methods, our project focuses on exploring the use of artificial substrate in the field of oyster restoration. Our overarching research question is the following: How can artificial substrate be used to study methods of oyster restoration in the Chesapeake Bay? In Part One of our research project we applied the methods of electrolysis mineral accretion to create artificial substrate, and explore its potential for usage as an artificial substrate. In Part Two of our research process we explored the methods of 3D printing to generate artificial substrate, which we later tested for oyster spat settlement success.

Part 1: Electrolysis Mineral Accretion

Introduction

The eastern oyster population in the Chesapeake Bay has declined drastically since the early 1800s, due to a variety of factors such as over-harvesting, disease, and habitat degradation. As the oyster population continues to decline, there are fewer and fewer natural reefs available for larval settlement and spat growth. To address substrate loss, many research and restoration efforts have focused on the creation of alternative materials on which oyster larvae may settle. However, many methods are costly and unsustainable in the long term.

This project proposes the utilization of electrolysis mineral accretion to explore the creation of a sustainable and energy-efficient oyster reef. Electrolysis mineral accretion has been successfully applied in previous experiments to stimulate the growth and repair of coral reefs. However, few studies have attempted to transfer this technology to oyster reef restoration and research, and none have done so in the Chesapeake Bay. This project proposes an innovative application of electrolysis mineral accretion by carrying out electrolysis in the lab and setting oysters prior to deploying the reef structure into the field in order to address issues faced by previous studies. Overall, the creation of an artificial oyster reef that utilizes the process of electrolysis mineral accretion has the potential to maximize oyster growth and reduce the effects of substrate loss.

A Review of Literature on Electrolysis Mineral Accretion

Electrolysis Mineral Accretion Background

One potential method to address declination of substrate in the Chesapeake Bay is electrolysis mineral accretion. Electrolysis mineral accretion is the application of an electric current to a substance or solution, causing anion and cation components in solution to precipitate out of solution at oppositely charged electrodes (Hilbertz, 1981). As energy is applied to the electrolyte field, reduction and oxidation reactions occur simultaneously. Electrical potential exists between electrodes, leading to a concentration gradient attracting negative ions to the positively-charged anode and positive ions to the negatively-charged cathode (Sabater & Yap, 2004). Precipitation of ions onto the submerged metal structures creates a coating of mineral substrate over the metal structures (Hilbertz, 1981). When electrolysis is applied to seawater, water molecules split at the cathode into hydroxide anions (OH^-) and hydrogen cations (H^+), which interact with other minerals in ocean water, including magnesium (Mg^{2+}), sulphur (S^{2-}), calcium (Ca^{2+}), potassium (K^+), bromine (Br^-), and carbon (Hilbertz, 1981). Mineral accretion specifically occurs as free floating calcium and magnesium ions combine with dissolved bicarbonate and hydroxide ions, respectively, to form $CaCO_3$ and magnesium hydroxide ($Mg(OH)_2$) (Sabater & Yap, 2004). As these ion gradients are realized, the pH surrounding the cathode increases, with the physical acceptance of hydrogen ions visible with the evolution of hydrogen bubbles from the cathode (Schuhmacher & Schillak, 1994). At the same time, the environment surrounding the anode becomes more acidic as hydrogen ions form, and oxygen molecules (O_2) and chlorine ions (Cl^-) are released from the water in gaseous form (Sabater & Yap, 2004).

The result of the electrolysis of seawater is the precipitation of molecular compounds, including calcium carbonate, magnesium hydroxide, hydrogen, oxygen and chlorine (Hilbertz, 1981). The resulting mineral material that forms on the cathode, which can be used to create a template for growth of reef organisms, is highly attractive to marine organisms due to the material's chemical and textural similarity to biogenic reef structures (Schuhmacher & Schillak, 1994).

In addition to generating substrate, electrolysis of seawater increases the bioavailability of mineral ions including calcium, magnesium, carbonate, hydroxide and bicarbonate, all ions needed for the natural process of calcification when oysters build their protective shells (Hilbertz, 1979). Calcification depends on the process of biomineralization and the dissolution of calcium carbonate to be used in biomineralization (Dickinson et al., 2012). During the process of biomineralization, the calcifying organism forms minerals such as calcium carbonate, calcium phosphate ($Ca(H_2PO_4)_2$), silicon dioxide (SiO_2), and iron oxide (Fe_2O_3) to grow its skeleton (Jackson & Wörheide, 2011). In the case of shelled mollusks, biomineralization is an essential stage in their life cycle because this is the process by which they form their outer shells (Hilbertz, 1979). Similarly, the natural process of calcification has been hypothesized to potentially allow oysters to invest less energy into their own calcification process and redirect energy distribution throughout their life (Gazeau et al., 2013).

Coral Research Efforts

The process of electrolysis mineral accretion was developed by Wolf Hilbertz in 1974 when he passed electric current through seawater as a method to study the formation of calcium carbonate-based shells and reefs (Goreau & Trench, 2012). Through further research, he found that calcium carbonate combines with magnesium,

chloride, and hydroxyl ions during this process, creating a mineral surface atop the cathode (Goreau & Trench, 2012). Hilbertz patented this method in 1979, which has since then been applied in various places around the world create sustainable coral reefs, predominantly in remote areas where the proper equipment and labor are unavailable (Goreau & Trench, 2012).

Biorock reefs are created by applying low-voltage electric current directly to a metal reef structure, typically made of rebar or metal mesh that is attached to the seafloor. After a few days, the mineral coating begins to develop, at which point divers descend to attach pieces of coral (Hilbertz, 1979). These coral fragments quickly bond to and grow on the mineral surface, since the continuous electric current supplies the appropriate ions for growth- namely carbonate ions (Hilbertz, 1979). Soon after, the electrolysis-created structure closely mimics a coral reef that would be naturally found in that ecosystem, as the corals continue to grow at a rate that can be up to five times faster than natural growth (Goreau & Trench, 2012). This faster growth rate is hypothesized to be due to the lower metabolic cost associated with the increase in pH surrounding the mineral precipitate (Piazza et al., 2009). Biorock is typically cost-effective, as it requires the energy source and rebar or mesh structure as the only materials. Further, most iterations of this technology are able to use renewable energy such as solar or wave energy to generate the electric current (Goreau, 2012).

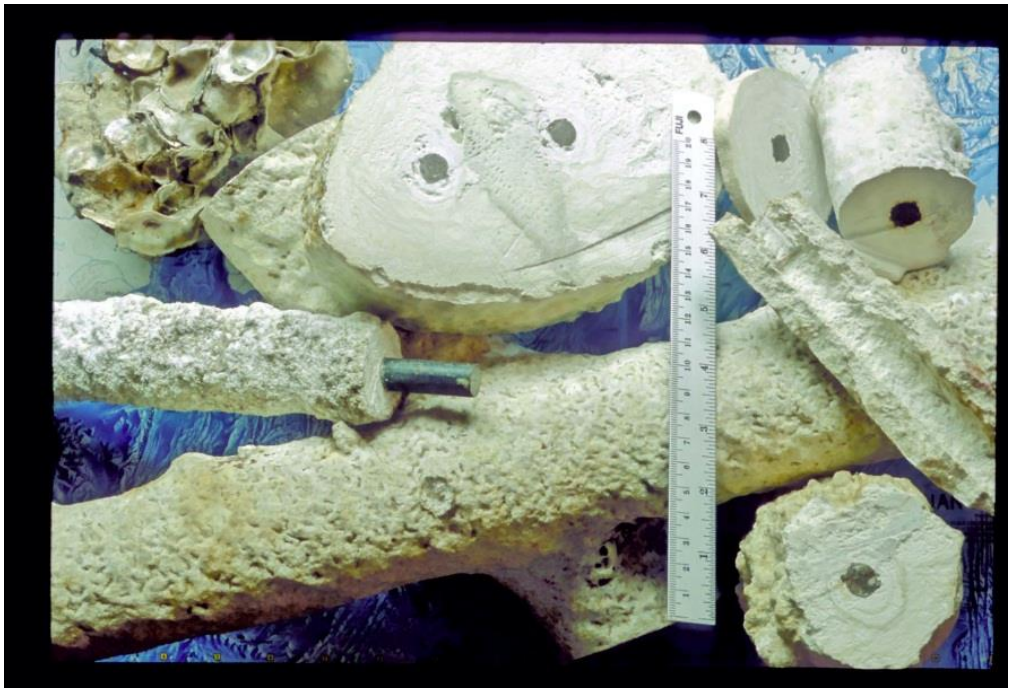

Figure 7: Biorock material sampled from various locations (Goreau, 2012).

Since its conception, the focus of electrolysis mineral accretion in research has been on coral restoration, as the Biorock technology has been employed in more than 20 countries around the world, offering vibrant coral reefs for a healthy local ecosystem, tourist attractions, and seashore restoration. A proven benefit of Biorock reefs is coastal protection. In 2004, a 50 m long Biorock reef was created off the shore of a severely degrading beach in the Maldives. The Maldives is a low-lying country in immediate threat from rising sea levels brought on by climate change. The Biorock reef employed off this beach consisted of a open framework design implanted with coral fragments (Goreau & Trench, 2012). Serving as a barrier from waves, this reef structure provided coastal protection soon after its implementation, and after a few years the beach grew 15 m (Goreau & Trench, 2012). Further, after a heat wave in 1998, the Biorock reef was found to have a coral survival rate 50 times higher than the natural reefs of the area (Goreau & Trench, 2012).

Oyster Research Efforts

Few studies have used electrolysis mineral accretion for oyster restoration and research. Piazza et al. (2009) used electrolysis mineral accretion on an artificial reef structure in Grand Isle, Louisiana to study eastern oyster recruitment and growth (Piazza et al., 2009). The purpose of this study was to compare oyster spat settlement and growth on an electrified reef off the coast of Louisiana with these same characteristics on a non-electrified reef (Piazza et al., 2009). The authors of this study did not find a significant positive impact of electrolysis conditions on eastern oyster spat settlement or juvenile growth, when compared to the non-electrified control reef; in fact, oyster spat seemed to prefer the control conditions, as the control bars had approximately twice as many oyster spat than the treatment bars (Piazza et al., 2009). These results were partially explained by flawed experimental design which concentrated the electrical current to one area of bare steel, preventing it from reaching the oysters at a sufficient rate to stimulate and sustain oyster growth (Goreau, 2014). Overall, this study was the first to investigate electrolysis mineral accretion in the Louisiana Gulf ecosystem using the eastern oyster, and concluded that further research into this process would be needed, hypothesizing that initial creation of mineral substrate in the lab followed by subsequent oyster settlement may be more beneficial for developing a successful oyster reef using electrolysis mineral accretion (Piazza et al., 2009).

Latchere et al. (2016) investigated the impact of electrolysis on the biomineralization of pearl oyster juveniles (Latchere et al., 2016). Pearl oyster juveniles in this study were grown under low-voltage electrolysis conditions for nine weeks in hatchery conditions. Throughout the experiment, juveniles were measured and weighed, and after nine weeks were analyzed using genomic techniques.

Researchers found a varied effect of electrolysis depending on the size of the juveniles, which were placed into small, medium, and large groups prior to the experiment. For example, electrolysis significantly increased the size of juveniles in the large group after 5 weeks for shell height and after two weeks for wet weight, but significant growth for juveniles in the medium group was delayed in comparison, with significant increases in shell height only occurring after the seventh week and wet weight after the ninth week only (Latchere et al., 2016). This research is unique in that it is the first to study the impact of electrolysis mineral accretion on the pearl oyster, as well as being the first study to use molecular approach to analyze biomineralization caused by electrolysis mineral accretion.

Shorr, Cervino, Lin, Weeks, & Goreau (2012) used the Biorock technology to carry out experimental stimulation to oyster reefs in New York City. Located adjacent to a former Superfund site previously used to build ships during World War II, the experimental site lacked a healthy natural oyster population, thus would be a good place to observe the effect of electrolysis mineral accretion on oyster settlement and growth (Shorr et al., 2012). In this experiment, eastern oysters were attached to Biorock reef structures as well as non-electrified control reefs and left to grow in the river. Overall, oysters on the electrified reef structures grew faster and became healthier than those under control conditions (Shorr et al., 2012). For example, over the wintertime period, which would typically be a dormant season for oysters, the electrified reef oysters showed survival rates of 66-100%, while the control oysters showed mortality rates of over 91%, with the survivors showing a clear decrease in length (Shorr et al., 2012). It is important to note that the electrified reefs were created with three voltage conditions: low, medium, and high, with oysters under the high

voltage consistently showing the highest growth rates and survival (Shorr et al., 2012).

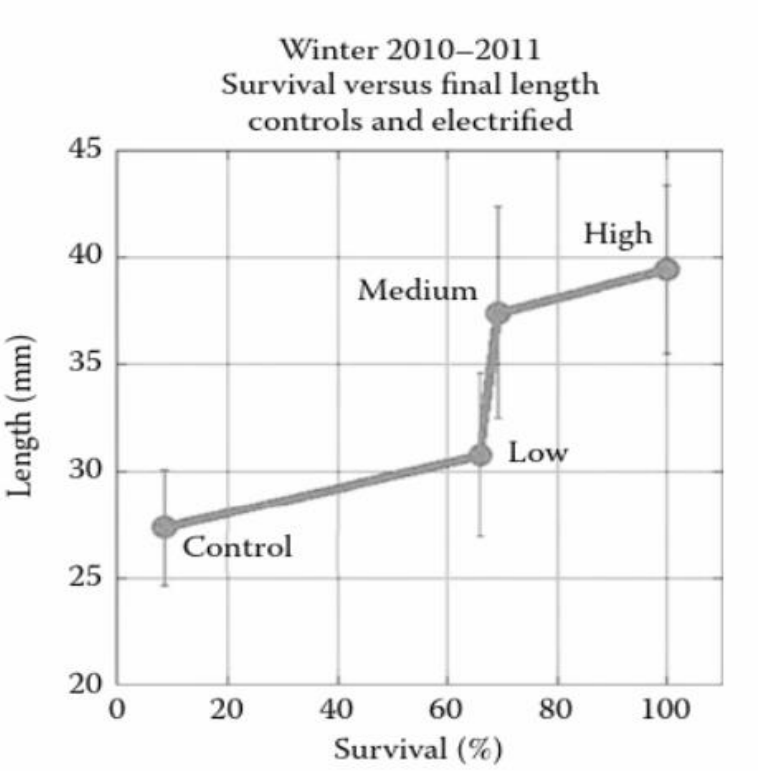

Figure 8: Survival and length increase as voltage increases. All electrified reefs show higher size and survival than the control reef (Shorr et al., 2012)

A 2014 research article by Goreau quantified the overall success of Biorock technology for reef restoration. He found that the application of low-voltage electrical current across electrodes in seawater increases coral settlement by 25.86 times when compared to non-electrified control reefs (Goreau, 2014). Additionally, the growth rates of corals, soft corals, oysters, and salt marsh grass is increased by an average of 3.17 times when compared to control reefs, and their survival is increased by a magnitude of 3.47 (Goreau, 2014). The improved settlement, growth rate, and survival documented in this review article are thought to be due to the electrical

stimulation of biochemical energy production pathways of these marine organisms (Goreau, 2014).

The literature on electrolysis mineral accretion provides a basis for our project. Currently, there have been no experiments conducted using electrolysis mineral accretion to study the eastern oyster in the Chesapeake Bay, nor have there been estuarine based experiments that utilize the technique described in the following sections.

Materials and Methods

Questions and Hypotheses

Electrolysis mineral accretion has been applied successfully to coral reef habitat, most recently making headlines for work in Tahiti in coalition with the hotel and tourist industry, as well as restoring eroding beaches in North Sulawesi, Indonesia (Kickham, 2019; Trialfhianty, 2017). Despite the success with coral reefs, there has been minimal experimentation with oysters. We sought to explore the use of electrolysis mineral accretion across a rebar structure in order to prompt calcium-based substrate growth in the lab, making this an original and unique endeavor. This substrate-coated structure could potentially be tested for spat settlement and growth to determine if this process would be a viable option for oyster restoration efforts in the Chesapeake Bay.

With this goal in mind, we created an overarching research question which would continue to guide our research for the entirety of the project: How can artificial substrate be used to study methods of oyster restoration in the Chesapeake Bay? To more specifically address this part of the project, we asked the following two questions: Can we use the process of electrolysis mineral accretion to create artificial

substrate? Is this substrate capable of supporting oyster spat settlement and oyster growth?

To address these research questions, the team created the two following hypotheses which were addressed in consecutive order: First, the process of electrolysis mineral accretion, under the proper conditions, will precipitate substrate containing $CaCO_3$ onto a rebar structure. Second, this substrate would be capable of fostering a significant level of oyster settlement and growth. The ideal conditions for electrolysis mineral accretion was to be determined by experimental testing and existing literature. Significance of of oyster spat settlement and growth could be tested by comparing oyster settlement, mortality, and growth between oyster shell substrate and minerally accreted substrate. However, due to insufficient results from the lab-phase electrolysis, we were unable to conduct oyster spat settlement and growth experiments, as is explained in the results section of this paper.

Laboratory Setup

The first phase of electrolysis mineral accretion testing took place in a laboratory setting, in the University of Maryland, Paynter Oyster Research Lab. We set up the experiment using two pieces of 0.5 inch by 1 foot long rebar as an anode and cathode, which were set parallel to each other, about half a foot apart within a one foot by two foot aquarium tank. Insulated copper wires were used to connect the rebar to a transformer, generating a circuit between the two pieces of metal. Salinity of the tank was prepared to 50 ppt using Instant Ocean Sea Salt, to mimic previous experiments utilizing electrolysis mineral accretion which had shown that a higher salt content may benefit the electrolysis process (Goreau, 2012; Zamani et al., 2010). Background research into previously used setups for electrolysis mineral accretion experiments led us to utilize transformer settings of 12 volts and 5 amps (Goreau,

2012; Zamani et al., 2010). Multiple trials were conducted with the transformer set to these settings, and let run between forty minutes to an hour, until the circuit appeared to deteriorate. The appearance of bubbles around the cathode was used as an indicator of the reaction initiating, as hydrogen bubbles are generated in the initiation of the oxidation-reduction reactions that occur during the mineral accretion process (Hilbertz, 1979). When the circuit appeared to deteriorate, we no longer observed the emission of hydrogen bubbles from the cathode.

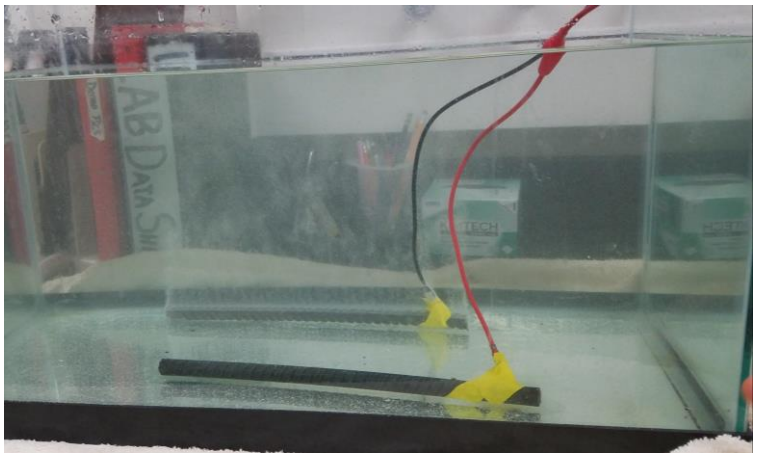

Figure 9: Lab set up for electrolysis mineral accretion settling. Anode and cathode circuit set up, connected to transformer via insulated copper wires. The red wire was connected to the anode, and the black wire was connected to the cathode. Hydrogen bubbling is occurring around the cathode in this image.

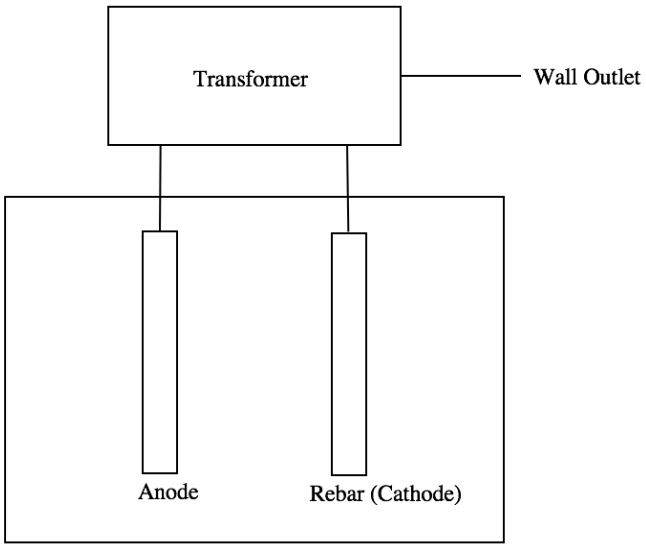

Figure 10: Diagram showing organization of anode and cathode in lab tank set up.

Open System Setup

After several trials of electrolysis mineral accretion testing in the lab setting did not produce desired yield levels of mineral accretion for oyster testing, we continued testing in an open water environment at the Eastern Shore Laboratory of the Virginia Institute of Marine Science (VIMS) during the summer of 2017. The open water set up was pursued as our results indicated that potentially a main factors inhibiting our outcomes were related to the limited source of water in the closed tank set up. A flow-through tank was used, where a cathode made of rebar and anode made of titanium were set on a crate to be deployed in a flow through tank with water source from the York River of the Chesapeake Bay watershed. Titanium, a less corrosive metal than rebar, was selected as the anode for this experiment after previous trials in the lab showed the rebar anode to corrode under electrified conditions.

The pieces of metal were held in place on a plastic crate by zip ties, and electrical tape attached the cathode and anode to insulated copper wires that were

connected to the transformer (Figure 11). The crates were one foot long by two feet wide. Both transformers were set to 5 amps. One was set to 12 volts, while the other to 16 volts, based on previous research open water settings (Goreau, 2012; Zamani et al., 2010). The experiment was left for a week, as previous experiments had taken approximately this amount of time for the buildup of accreted mineral material to occur. After one week, the materials were retrieved for observational data collection. Data on the Eastern Shore Laboratory (ESL) water quality was obtained from the ESL water quality monitoring station of VIMS.

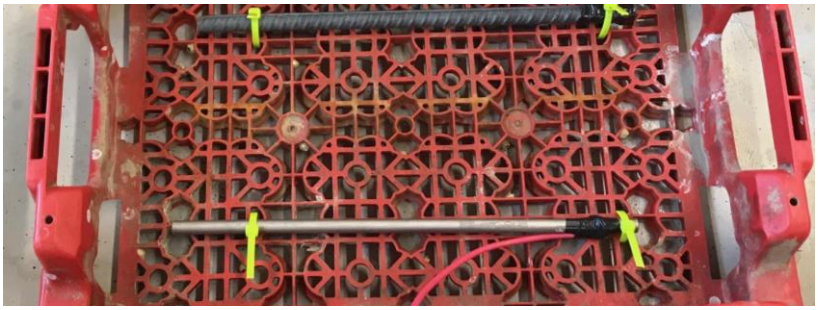

Figure 11: Flow through tank set up. A titanium rod was used as the anode, and a piece of rebar was used as the cathode.

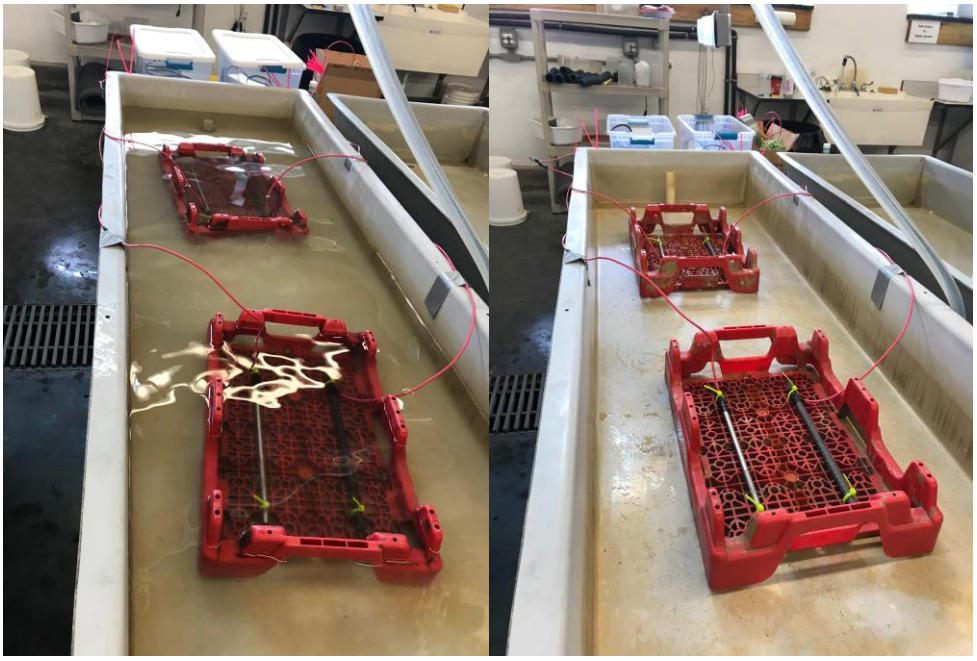

Figure 12: Experimental set up at VIMS. Here both flow through tank experiments were set up adjacent to each other in the same tank to ensure identical experimental conditions. Water in the tank was pumped from the York River, located next to the laboratory.

Results

Laboratory Setup

In the laboratory experiments, we observed electrolysis with the visible release of oxygen bubbles around the cathode, and the precipitation of mineral particles on the anode. Five trials were conducted that resulted in minimal accumulation of mineral precipitate. The only visible precipitation were small white particles that flaked off of the rebar when touched. Soft, white precipitate within the solution was also observed during the electrolysis experimentation, however, the precipitate did not settle on the pieces of rebar and, rather, settled on the floor of the tank. The volume of precipitate was deemed too little to be captured for further analysis.

One unanticipated result of electrolysis mineral accretion experimentation, and appeared to be related to the oxidation reactions, was the observation of color change

of the tank solution as components of the rebar precipitated into the tank solution. Color change occurred almost immediately as hydrogen bubbling occurred, starting with a yellow color that continued to darken to green and then black, as precipitates within the tank solution accumulated, until the tank achieved zero visibility, sometimes with dark particles floating on the top. After forty minutes to an hour, hydrogen bubbling ceased, at which point the experiment was deduced to have stopped. Upon removal of the pieces of rebar from dark solution we was observed that the connecting copper wires had corroded off of the transformer clasps and therefore accounted for the termination of the redox reactions. Additionally, the voltage and amp settings on the transformer had changed, such that the voltmeter read 0 volts and 5 amps. This change occurred independently, appearing to occur as a result of the circuit breaking due to the corrosion of the connecting wire.

After removal from the tank, the cathode was physically unchanged despite the presence of a small amount of mineral, while the anode had visibly deteriorated; the presence of melted precipitate, in a form of a soft black sludge on top of the surface of the rebar (Figure 15). After two trials with these results, we changed the anode material to stainless steel, a less corrosive metal, however, this modification did not change the outcome in further trials. The magnitude of mineral accretion that was achieved in a lab setting was found to be overall too small relative to the hypothetical amount needed for our project. While our project wasn't able to produce our initial goal of mineral accretion for oyster testing, lab testing electrolysis was found to be successful in effectively inducing the process of mineral accretion.

Figure 13: Tank coloration through lab-tank experiments. This shows the color change that accompanied the electrolysis experimentation in the closed system set up in the lab. The color change was attributed to the dissolution of the rebar anode as the circuit was applied to the system.

Figure 14: Mineral accretion in the closed tank setup. The mineral that precipitated were small white particles that appeared to flake off when touched. It is unclear if the mineral layer achieved was calcium carbonate, however this does show potential positive results.

Figure 15: The anode rebar in the closed tank set up. The anode seemed to degrade slightly after exposure to electricity, as is visible in this picture the metal. This posed a potential limit in the lab-tank experiments, as the anode dissolution led to saturation of the tank solution with rebar components and led to the corrosion of the connective wire.

Open System Setup

The following graph shows characteristics of the flow-through water from the Eastern Shore Laboratory water monitoring stations, which came from the York River of the Chesapeake Bay Watershed. Changes in water quality were found to occur based on hour of the day, and naturally cycle. On average, the water characteristics remained at an overall uniform profile during the time of experiment. Overall, the water quality throughout the week of experimentation was fairly consistent with the exception of values of pH changing with time of day.

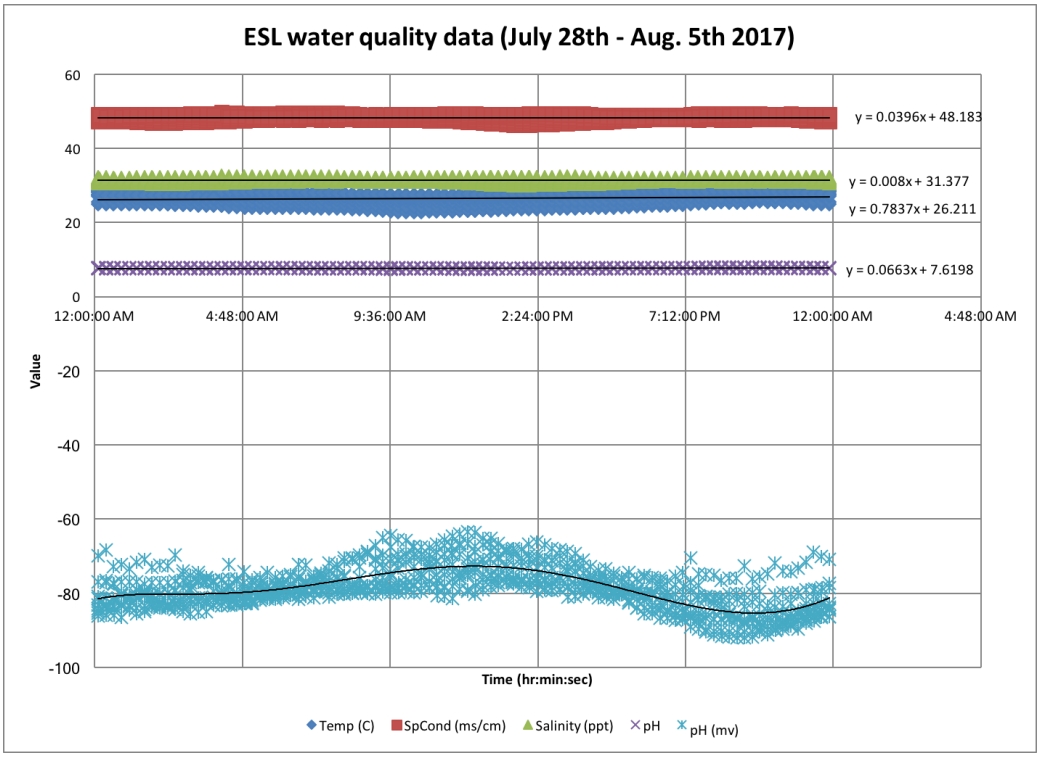

Figure 16: Water Quality Data during Electrolysis Testing at VIMS

After one week of open-system experimentation, the pieces of rebar obtained a thin layer of mineral accretion where they had been exposed to water. The coating was measured to be 1 mm in width, giving an estimated volume of $4.176 * 10^{-6} m^3$.

Volume was calculated as the volume of a cylinder (rebar structure) with the coating, minus the internal volume of the rebar bar using the following formula: $V = \pi r^2 h$. The rod was measured to be 1 foot long (0.3048 meters), radius of the rebar was 0.25 inches, and radius including the final mineral accretion level was 7.35 mm (0.25 inches* (25.4 mm/1 inches) + 1 mm =7.35 mm*10^{-3} m/mm= 0.00735 meters). The final volume (V_F) including mineral accretion was estimated using the following calculations: $V_F = \pi * (0.00735\ m)^2 * 1\ ft\ (0.3048\ m/\ 1ft) = 1.64660581 * 10^{-5} m^3$. Initial volume of the rebar (V_I)was estimated by the following calculation: $V_I = \pi * (0.00635\ m)^2 * 1\ ft\ (0.3048\ m/\ 1ft) = 1.2290298 * 10^{-5}\ m^3$.

Volume of mineral accretion was estimated by the following calculation: $V_F - V_I = V_m$, where V_m is the final volume of mineral accretion that was achieved: $V_m=(1.64660581* 10^{-5}m^3)- (1.2290298* 10^{-5} m^3)=4.1757601* 10^{-6}m^3$.

The mineral was a white material that was relatively hard compared to the previous laboratory experiments. At the time of data collection, bubbling, an indicator of redox reactions occurring, had ceased, indicating that the mineral accretion process had stopped. This appeared due to the fact that the copper wire connecting the transformer to the rebar had corroded and come off of the rebar, and that the titanium anode had partially dissolved. Upon retrieval, the parts of the titanium pieces had broken apart from the original structure, and contained build up of a soft white mineral surrounding the broken apart pieces. At the time of data collection, the two transformers read (12 volts, 0 amps) and (16 volts, 0 amps), indicating that the circuit no longer was functional.

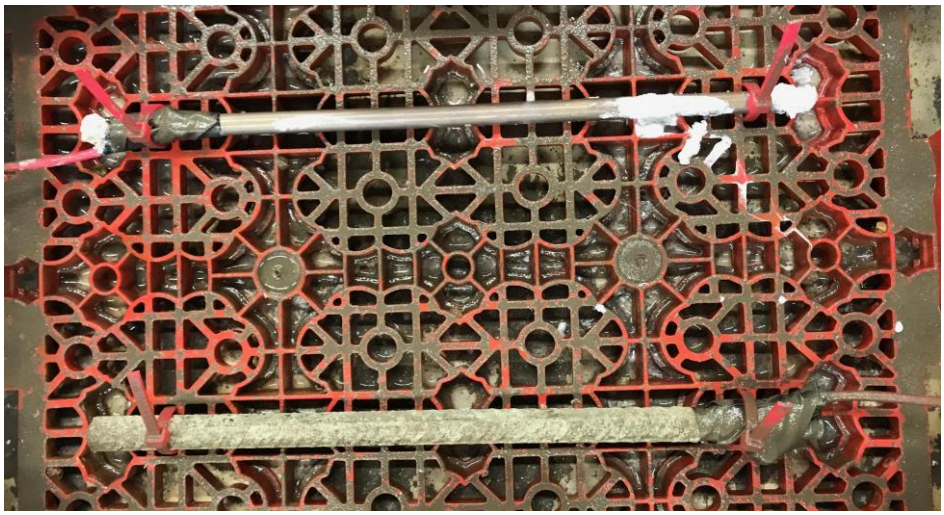

Figure 17: ESL flow through tank results. The flow through tank from the Eastern Shore Laboratory experiments results in full coverage of the cathode (bottom) in white precipitate, indicating successful mineral accretion. Visible in this image is corrosion of the titanium anode (top), which is thought to have been a limitation in achieving further accretion on the cathode.

Figure 18: Mineral accretion on the cathode. Close-up view of the mineral accretion results on the cathode. As is observable in the image on the right there is a substantial difference in mineral accretion achieved on the exposed segment of the cathode verses the unexposed rebar (black).

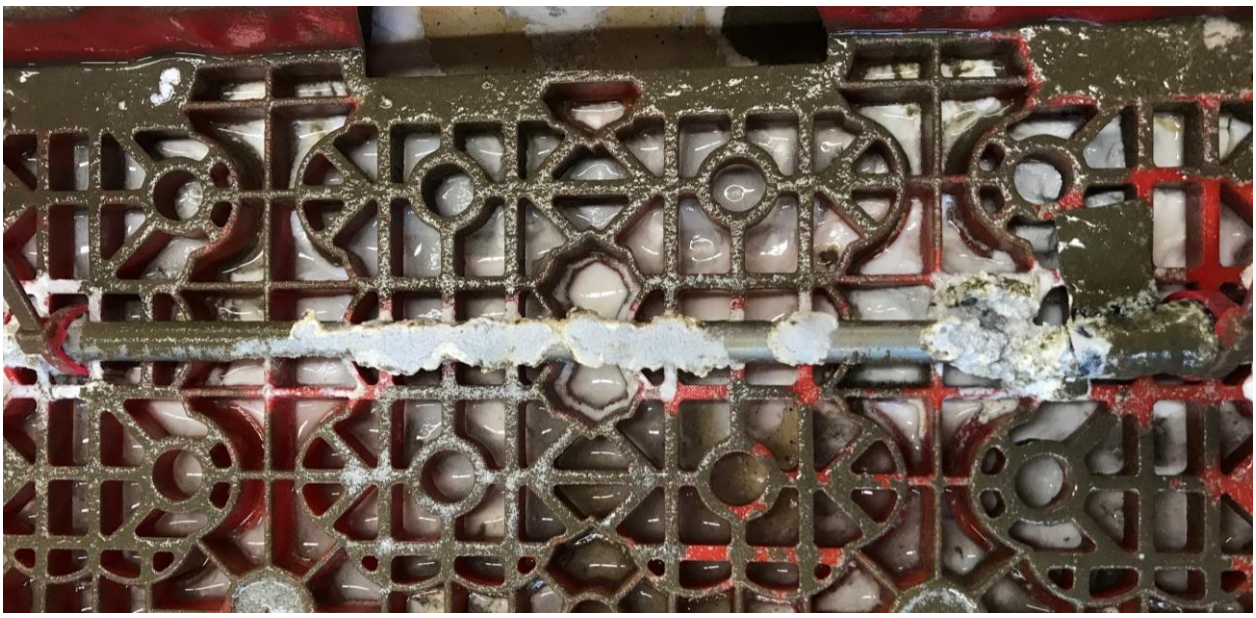

Figure 19: Corrosion of the titanium rebar that occurred as the experiment progressed. The piece of titanium connected to the transformer (right side) corroded off the larger

piece of titanium, breaking the circuit and likely posing a limit to achieving increased levels of mineral accretion.

Discussion

Throughout the electrolysis experiments, the closed system and transformer appeared to pose a limitation to successfully achieving accumulation of mineral accretion substrate. One limitation in achieving substantial mineral accretion was the transformer, which was unable to achieve a constant set voltage and amperage throughout the duration of the experiment. Voltage would increase starting below 12 volts (around 5 or 6 volts), and decrease or oscillate if amperage remained constant. During one experiment, the transformer reached 12 volts, but only after amperage decreased to zero. This can be partially explained by the corrosion that occured over time to the connective wire. Once the connective wire was severed, the constant flow of electricity could no longer be maintained. Additionally, since the experimental set up required the use of electrical tape, it was difficult to observe when this corrosion would be occurring and effective in limiting the electrical flow, and therefore it was unlikely that this error could be corrected at the time that it might occur. Similarly, the use of rebar and titanium as anode material may have been a limit, as the corrosion of these metals might have restricted the continuation of mineral accretion. The changes in coloration in the closed tank set up appeared to be related to the corrosion of the pieces of rebar as the circuit was applied to the system and therefore, would account for decreased electrolysis reactions as the experiment continued. Overtime, we would eventually expect to see the experiment cease, as all conductible elements of the rebar were dissolved.

The use of a closed system, in which electrolyte composition and ionic compounds differ from an open system, may have been another potential limitation to

achieving the desired level of calcium carbonate (Hilbertz, Fletcher, & Krausse, 1977). In a closed system, there is potential that structural development is inhibited if high enough solution alkalinity levels are reached, such that brucite ion will exceed the solubility product and, therefore, over-saturate the rebar structure. Additionally, in the event that amorphous matter envelopes the cathodes or there is the presence of other crystals including hydroxides, phosphates or sodium carbonate in the water, structural development atop the rebar may be prevented (Hilbertz, Fletcher, & Krausse, 1977).

Both the open water and closed tank experiment did not involve continuous observation, and data was only collected at the start and end of the experiment. As a result, the main limiting factor in these trials is unknown as all of these factors might have played a role. The success of the open-water flow through tank experiment indicated that the process of electrolysis mineral accretion provided a viable method for artificially inducing the production of mineral accretion, that could be potentially applied for oyster spat restoration. The deposition on the rebar from the field testing was too thin however for potential oyster spat experimentation. Additionally, once the semester started, and members of the team returned to campus, we were unable to access the outdoor flow-through tanks and repeat the experimentation using flow through tanks. The mineral produced in this experimental set up was deemed too thin for any potential oyster spat experimentation, which is why the resulting mineral produced in the open water set up was not analyzed further with the application of oyster spat. If this experiment were repeated, future testing would be beneficial to allow for the analysis of the mineral components.

Future Directions

The preliminary results from this project indicate the potential of electrolysis mineral accretion to add significantly to oyster restoration efforts in the Chesapeake Bay. Electrolysis mineral accretion in the Chesapeake Bay has potential be an efficient technique for producing artificial, self-sustaining reefs that closely mimic the naturally-occurring calcium carbonate reefs preferred by oysters. These oyster reefs have the potential to assist in population restoration as well as rehabilitation for other marine organisms that rely on the source of food and habitat provided by the reef. From the limited results of this project, it is clear that more research is needed to determine the ideal conditions for promoting electrolysis mineral accretion in a lab setting. Future researchers are encouraged to look at different materials for the cathode and anode, specifically the anode, which proved to be limiting as the titanium deteriorated over the course of the open water experiment. Similarly, the use of more durable electrode tape and electrode connecters would likely result in a longer duration of the electrolysis experimentation. Overall, we find that our results indicate that electrolysis provides a potential mechanism for generating attractive alternative oyster reefs structures. Standardized methods for this process should be created in order to provide researchers with the most efficient and successful steps to achieve the formation of calcium-containing substrate onto a metal structure.

Part 2: 3D Printing

Introduction

This section of the research seeks to combine additive manufacturing with the previous research on oyster restoration. The team experienced a merger one year into research, with four new members joining from a team focused on 3D printing. To best optimize team member expertise, we decided to focus on oyster shells, which combine biology and engineering. The team proposed using additive manufacturing techniques to create oysters shells for spat settlements and growth.

A Review of the Literature on the Use of 3D Printing

Polymer Printing Technologies

Introduction.

3D printing began as a method for rapid prototyping and has been praised for its accessibility and ability to produce complicated geometry. There are multiple printing processes, including Fused Deposition Modeling (FDM), Stereolithography (SLA), Digital Light Processing (DLP), polyjet printing, inkjet printing, and Selective Laser Sintering (SLS). The stereolithography apparatus was the first additive manufacturing design, but FDM is more commonly used due to the lower capital investment, less expensive materials, and safety risks. Each process holds major advantages over the others, while at the same time has limitations affecting their overall accessibility, performance, and applicability.

Methods.

Fused Deposition Modeling (FDM) is the most accessible, low cost additive manufacturing method currently available. In an FDM printer, rollers feed plastic filament into a heated nozzle, which melts the filament and deposits it onto the build

plate as illustrated in Figure 20. Stepper motors dictate the position of the nozzle in the horizontal plane. The stage moves down after each layer until the print is finished (Gross, Erkal, Lockwood, Chen, and Spence, 2014). After the print is complete, the user removes the part from the print bed and breaks away the plastic support material.

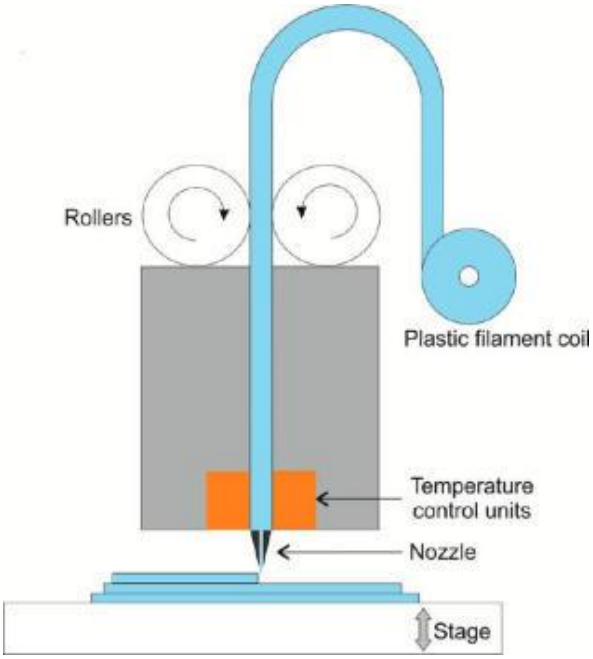

Figure 20: In FDM printing, filament is pushed through the extruder by rollers, into a heated nozzle. The heat liquefies the filament for extrusion and then it quickly solidifies on the build plate. Retrieved from Gross et al. (2014).

The stereolithography apparatus (SLA) was developed by Charles Hull and played an instrumental role in commercializing 3D printing (Gross et al., 2014). The process centers around a resin that solidifies in the presence of ultraviolet (UV) light. The application of the UV light, as well as the placement of the stage, led to the formation of two separate subprocesses. In the most common form of stereolithography printing, a concentrated beam of UV light strikes a mirror and is reflected onto a single point of the build plate. Two servo motors rotate the mirror, targeting the laser on other sections of the build plate and resulting in a path of partially cured resin. After the first layer is complete, the build plate translates a set

distance away from the light source and new layers are constructed on the solidified material. Once the part is generated, the operator removes it from the build plate, wipes away excess resin, and places it under UV light to complete the curing process.

The second photopolymer printing method, known as Digital Light Processing (DLP), replaces the single mirror with a digital mirror. The digital mirror uses a grid of reflectors whose orientations are controlled by electromagnets. When an electromagnet is on, the associated reflector directs light through a lens so that it strikes the build plate and causes photopolymer resin to cure at a single point on the build plate. Each electromagnet can be turned on or off to control the layer geometry. Unlike the scanner, the digital mirror allows the laser to solidify the entire layer at once, speeding up the process.

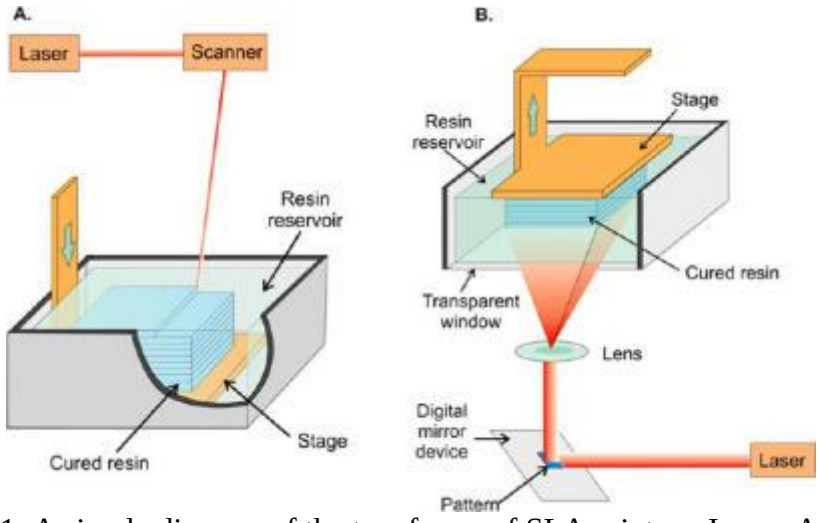

Figure 21: A simple diagram of the two forms of SLA printers. Image A shows a stage in place at the bottom of a resin tank with a laser focused onto the resin to solidify it. Image B shows the stage starting at the top of the tank with a laser reflecting off of a digital mirror to solidify the resin. Retrieved from Gross et al. (2014).

Photopolymer jetting, or polyjet, is a versatile technique in which one or more inkjet printheads deposit liquid photopolymers onto a build platform. Immediately after the layer is deposited, UV lamps cure the photopolymer. The build plate moves

down a set distance and a new layer is deposited on top of the existing material. In most polyjet printers, one printhead contains a dissolvable photopolymer, which is used as support material and can be easily remove after printing via a chemical bath. In some cases, a printer can deposit multiple non-dissolvable photopolymers together, allowing diverse material properties such as varying color, flexibility, and opacity. Furthermore, functionally graded materials are possible as the technique for exceptional accuracy and surface finishes.

3D inkjetting is a method for developing relatively low cost custom components. In this process, the bed plate is covered with a thin layer of polymer powder. As shown in Figure 22, an inkjet device, referencing the stereolithography file uploaded to it, moves around and drops a binding agent onto the powder, causing the plastic granules to fuse together (Gross et al., 2014). After every layer is finished, the stage drops down, and more powder is rolled onto the stage.

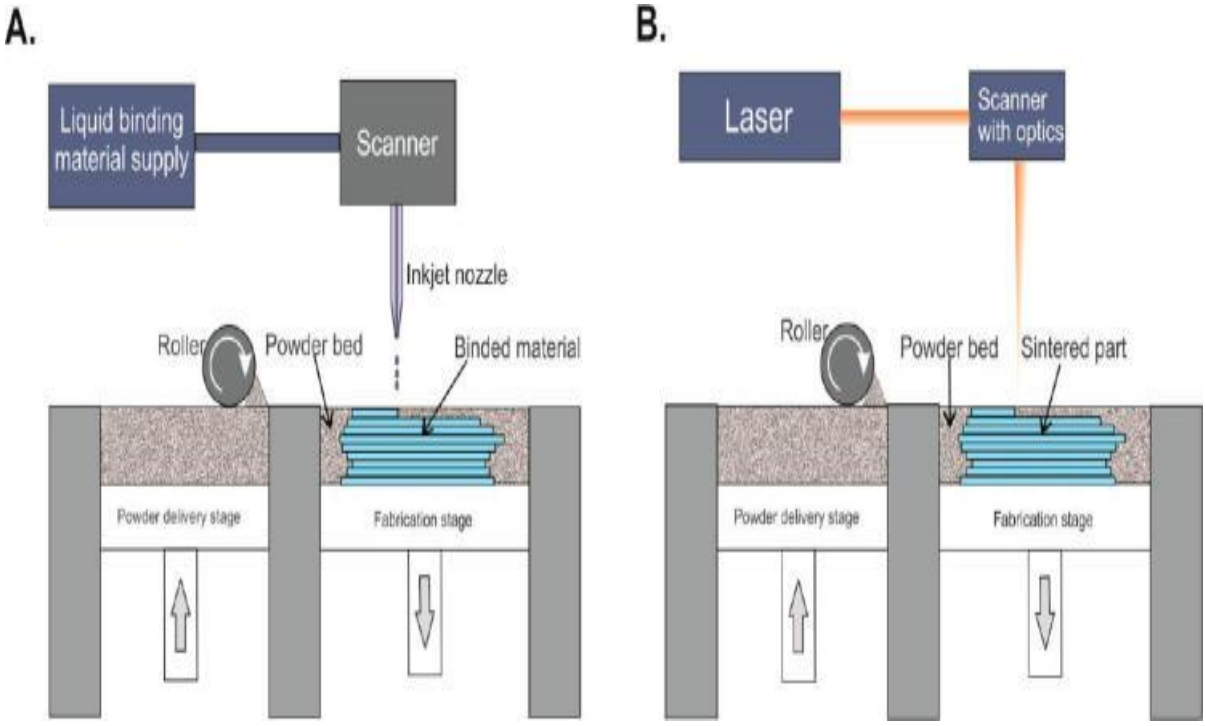

Figure 22: Inkjet printing where powder is rolled onto the stage and the liquid binding agent is dropped onto the powder to make it congeal. Then the stage is lowered and the process repeats for the next layer. Retrieved from Gross et al. (2014).

Selective Laser Sintering (SLS) uses a powder-based medium for printing, similar to inkjet 3D printing. However, this method obfuscates the need for a binding agent by selectively melting the powder. The build chamber is heated to just below the polymer's melting point and a laser is directed at coordinates identified by the slicing software. The laser increases the local temperature, causing nearby polymer grains to melt and fuse to one another. The laser traces out a path at each layer and the build plate moves down slightly, similar to the process in FDM.

Advantages and limitations.

While SLA and DLP are very similar processes and can both produce high resolution products, each has a few advantages over the other. SLA produces a smoother finish because the layer moves traces a continuous curve, whereas DLP relies on pixels. SLA also permits easy to remove supports and is more suitable for large high resolution prints. In contrast, DLP excels at producing large, low resolution prints or small, high resolution prints quickly (Formlabs, 2017). This subprocess also uses less resin, and allows for more height (Gross et al., 2014). Since SLA and DLP rely on the same photopolymer resins, the products from both processes are brittle and can suffer excessive shrinkage or warping upon solidification. The uncured resins also pose environmental risks and health risks including dermal and respiratory irritation.

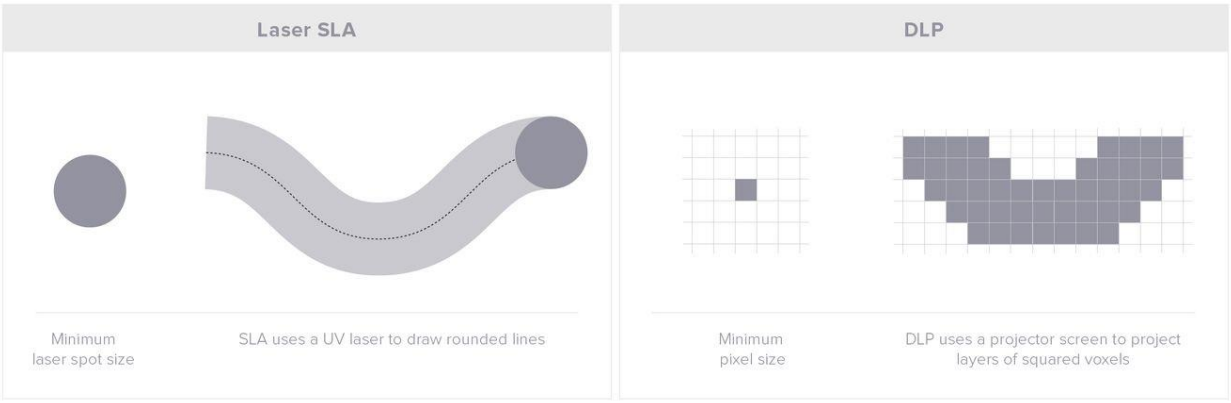

Figure 23: Comparison of layer geometry for SLA and DLP. Retrieved from Formlabs (2017).

Since polyjet printing can deposit an entire layer at once rather than tracing out individual curves, it is among the fastest printing methods. Photopolymer blending permits functionally graded materials. Polyjet printers are also known for high resolution and dimensionally accurate parts. However, polyjet printing is restricted to UV active polymers, which results in low strength, non-durable products that are typically only used for prototyping purposes and ergonomics testing.

Since inkjet 3D printing uses powders, the materials available to print with increased extensively (Gross et al., 2014). The spare powder also helps act as a support for the rest of the design, allowing the printer to print abstract designs at unorthodox angles without sacrificing a uniform surface. While the powder is a vast improvement over the resin, the print is overly dictated by the properties of the binding agents. This means that the product is still much weaker than a geometrically identical part made of the pure polymer. Another serious problem with binder jet printers is that not all the powder may congeal, creating porous interiors and rough outer shells for designs (Gross et al., 2014). The porous interior reduces the overall strength and a rough exterior may result in stress concentrations, making binder jet object unsuitable for high stress applications.

Melting the polymer obfuscates the binding agent, generating stronger products with more consistent material properties than achievable with ink jetting. Additionally, SLS can operate on a wider variety of polymers than inkjetting, since bonding depends on the thermal properties of the polymer, rather than the chemical compatibility of the polymer and the binding agent. While increased strength and material selection are crucial advantages, SLS prints can suffer major shrinkage and warping due to thermal stresses (Gross et al., 2014).

Fused Deposition Modeling (FDM) is often touted as the most accessible additive manufacturing method due to low capital investment, low material cost, and minimal training requirements compared to other techniques. Additionally, some FDM devices support multi-material printing, One huge benefit to FDM is that multiple materials can be used for one design (Gross et al., 2014). However, FDM components are anisotropic, as the extruded filament will not fuse completely with the previous or adjacent layers.

3D Scanning Techniques

3D scanners are extraordinarily useful tools for generating digital models of objects that cannot be easily modeled using traditional Computer Aided Design (CAD) software. There are several different scanning techniques available, including time of flight scanning, photogrammetry, laser triangulation scanning, and structured light.

Time of flight.

Time of flight scanning devices emit a beam of light onto an object and measure the time that passes before the reflection strikes the sensor. Since the speed of light is constant within a medium, the time difference can be used to precisely measure the distance between the scanner and the target object. Time of flight

scanners are often used for topography studies due to their high accuracy over long distances. They are also used in motion detection and tracking because there is minimal delay between processing the previous data set and receiving new information. However, time of flight scanning is highly sensitive to the accuracy and precision of the time measuring device, resulting in low quality data when the scanner is close to the target object.

Triangulation methods.

Using methods such as photogrammetry and laser triangulation, rather than time of flight, can often generate higher quality scans for close range applications. In photogrammetry, the user takes numerous pictures of a stationary three dimensional object from different positions, ensuring that there is some overlap between each image (Stachniss, 2015). The user then loads the images into a photogrammetry software, which uses color data and feature detection to select a series of points that two or more images have in common. Features such as edges are often identified based on sudden changes in the intensity of incident light (Stachniss, 2015). The software uses a process known as triangulation, in which it analyzes the distances between the selected points in each image to resolve the position of the camera relative to the object for each individual scan (see Figure 24). Then, the program can align each image to produce a composite scan of the entire object. The user can remove any undesirable points, including noise and data from the background. Since there may be minor differences in the position of pixels between images, most programs perform a least squares regression or similar estimation method to improve alignment.

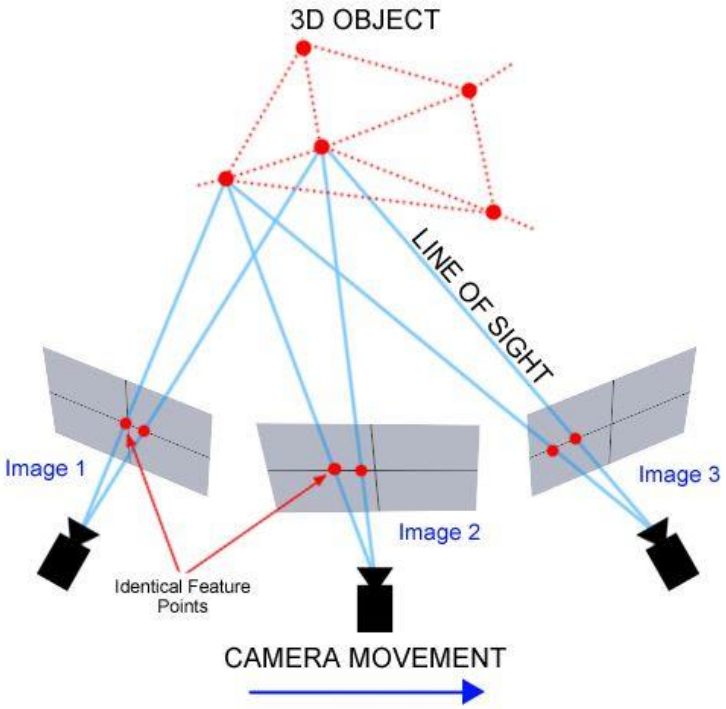

Figure 24: Triangulating positions for a photogrammetric scan (Mason, n.d.).

Similar to photogrammetry, laser scanners use geometric relationships to resolve the position of the object relative to the scanner. Laser scanners illuminate a single vertical or horizontal section on the target object and photograph it using a camera with a slight angular offset from the laser, as depicted in Figure 25. As the distance between the object and laser changes, the location of the light incident on the sensor surface will vary, enabling the software to resolve the distance between the camera and the illuminated section of the object (Movimed, n.d.). The laser gradually scans the object, generating a complete view of the surface. If multiple scans are required to capture the entire object, the user can stitch them together through the same methods used in photogrammetry in the scanning software.

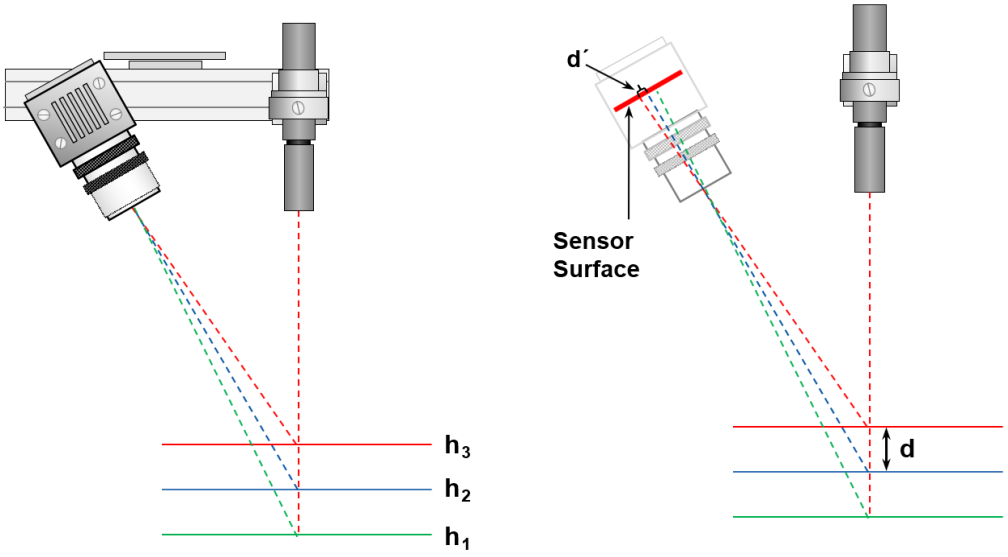

Figure 25: The distance between the laser and object surface influences where the the camera's sensor detects the beam of light (Movimed, n.d.)

Structured light.

Unlike photogrammetric and laser scanning, structured light techniques do not use feature detection in order to align the scans. Instead, a light pattern is projected onto the target object and one or more cameras photograph the object (Lopez et al., 2017). Since the geometry of the object distorts the width of each piece of the pattern, the software can identify the distance between the camera and the object at various locations, then construct a point cloud. The item is rescanned from various positions and the user matches overlapping geometry on each scan, generating a composite point cloud that represents the complete object.

RP techniques for bone scaffold fabrication.

Technique	Process details	Processed materials for bone tissue engineering	Advantages (+) and disadvantages (−)	Reference
3D Plotting/direct ink writing	→ Strands of paste/viscous material (in solution form) extrusion based on the predesigned structure → Layer by layer deposition of strands at constant rate, under specific pressure → Disruption of strands according to the tear of speed	→ PCL → Hydroxyapatite (HA) → Bioactive glasses → Mesoporous bioactive glass/alginate composite → Polylactic acid (PLA)/polyethylene glycol (PEG) → PLA/(PEG)/G5 glass → Poly(hydroxymethylglycolide-co-ε-caprolactone) (PHMGCL) → Bioactive 6P53B glass	+: → Mild condition of process allows drug and biomolecules (proteins and living cells) plotting −: → Heating/post-processing needed for some materials restricts the biomolecule incorporation	[32–38]
Laser-assisted bioprinting (LAB)	→ Coating the desired material on transparent quartz disk (ribbon) → Deposition control by laser pulse energy → Resolution control by distance between ribbon/substrate, spot size and stage movement	→ HA → Zirconia → HA/MG63 osteoblast-like cell → Nano HA → Human osteoprogenitor cell → Human umbilical vein endothelial cell	+: → Ambient condition → Applicable for organic, inorganic materials and cells → Quantitatively controlled → 3D stage movement −: → Homogeneous ribbons needed	[39–42]
SLS	→ Preparing the powder bed → Layer by layer addition of powder → Sintering each layer according to the CAD file, using laser source	→ PCL → Nano HA → Calcium phosphate (CaP)/poly (hydroxybutyrate–co-hydroxyvalerate) (PHBV) → Carbonated hydroxyapatite (CHAp)/poly(L-lactic acid) (PLLA) → PLLA → β-Tricalcium phosphate (β-TCP) → PHBV	+: → No need for support → No post processing is needed −: → Feature resolution depends on laser beam diameter	[43–48]
SLA	→ Immersion of platform in a photopolymer liquid → Exposure to focused light according to desired design → Polymer solidifying at focal point, non-exposed polymer remains liquid, → Layer by layer fabrication by platform moving downward	→ Poly(propylene fumarate) (PPF)/diethyl fumarate (DEF) → PPF/DEF-HA → PDLLA/HA → β-TCP	+: → Complex internal features can be obtained → Growth factors, proteins and cell patterning is possible −: → Only applicable for photopolymers	[49–52]
FDM	→ Strands of heated polymer/ceramics extrusion through nozzle	→ Tricalcium phosphate (TCP) → TCP/polypropylene (PP) → Alumina (Al_2O_3) → PCL → TCP/PCL	+: No need for platform/support −: → Material restriction due to need for molten phase	[26,30,31, 53–58]
Robotic assisted deposition/ robocasting	→ Direct writing of liquid using a nozzle → Consolidation through liquid-to-gel transition	→ HA/PLA → HA/PCL → 6P53B glass/PCL	+: → Independent 3D nozzle movement → Precise control on thickness → No need for platform/support −: → Material restriction	[59]

Figure 26: Table listing different methods of bone recreation via additive manufacturing. Retrieved from Bose, et. al. (2013)

Current Biological Uses of 3D Printing

Within the last several decades, additive manufacturing technologies have been gradually integrated into environmental research. Researchers have used FDM to produce parts for Autonomous Underwater Vehicles (AUVs) that resemble stingray (Barngrover, 2011). This design reduces drag when compared against traditional AUVs and allows the robot to hover and glide, which is useful for monitoring ecology. FDM and SLA have also been used in tandem with 3D scanning to replicate

the geometry of various organisms for researching hydrodynamic forces (Skavicus and Ditsche, 2014; Bartol, Gordon, Gharib, Hove, Webb, and Weihs, 2002).

In addition to environmental monitoring and fluid dynamics, additive manufacturing has made its way into restoration efforts. Dr. J. B. Gardiner and Sustainable Oceans International (SOI) manufactured reef structures using a binder jet printer with a material similar to sandstone (Gardiner, 2011). SOI and Gardiner's structures were deployed near Bahrain and Australia (Sustainable Oceans International, 2012). The Reef Design Lab has also used additive manufacturing, in conjunction with slip casting, to produce modular reef structures in the Maldives (Goad, n.d.).

Alongside ecological studies, additive manufacturing has recently entered the biological and biomedical fields, encouraging the development of fully biocompatible materials. Most of the existing research is centered around the human body instead of flora or other fauna. For example, tissue samples are taken from patients and then printed into various necessary organs (Gross, Erkal, Lockwood, Chen, & Spence 2014). Bone and teeth can also be recreated via various additive manufacturing methods. Researchers are using FDM to print with TCP and alumina, two compounds used in bone recreation (Bose, Vahabzadeh, & Bandyopadhyay, 2013). FDM is proven to be effective, but so far only in biomedical applications. Very little research exists on the use of additive manufacturing with other species. One such reason is that 3D printing is still in its relative infancy, so most research is still ongoing. Given its popularity and ubiquitousness, it would be beneficial to translate use of FDM to more than just bone restoration.

Materials

While seeking out suitable materials for creating the artificial substrate, the team identified an FDM filament known as LAYBRICK. The filament consists of approximately 50% $CaCO_3$ by weight, along with copolyesters and plasticizers (Hyrel 3D, 2016; Parthy, personal communication, Nov 4, 2017). The team ultimately selected this material, hypothesizing that the high calcium carbonate content would make it suitable for spat settlement. The material was classified as posing no risk to water pollution under Germany's classification system and had no known ecotoxicological effects at the time of approval (CC Products, 2015).

Settlement Cues

Settlement cues are any factors that stimulate larvae to settle on a substrate surface, usually the oyster shell. These can be physical factors, including anything from shell size to microtopography. Also, biochemical cues from the oyster shell or environment can incite settlement. 3D scanning and printing make replication of natural shells' physical cues achievable while voiding any biochemical component. 3D printed shell replicas can be used as blank models to examine the effectiveness of the physical shape of the oyster shell as well as various biochemical cues that can be applied to its surface.

Physical cues.

The shape of an oyster's shell can vary by the oyster's genetics or environment. The eastern oyster is a bivalve mollusk, so it has two hard, pear-shaped shells hinged together. The eastern oyster has evolved its shell shape to best survive the rough-waters and dangerous predators of the seafloor.

While settling on natural shells is most advantageous to oyster survival, spat is also known to settle on various other substrates of varying shapes and compositions.

For instance, in hatcheries, ceramic tiles are often used as proxy settlement surfaces when shells are not available (Metz, Stoner, & Arrington, 2015). In some cases, oysters settle on these square tiles at equal rates as natural shells (Metz et al., 2015). In settlement research, tiles may even be preferential because they allow spat to be counted per unit area (Metz et al., 2015).

A group of Brazilian researcher examined the settlement of mangrove oysters on differently shaped substrates (Nalesso et al., 2008). They found that the oysters prefer to settle on their natural shells, but will also settle on square tiles, rubber tires, and plastic bottles (Nalesso et al., 2008). These results show there is a physical component to spat settlement. Another team found that eastern oysters have a significant preference for limestone over sandstone and hypothesize the different is due to their differences in structure (Soniat & Burton, 2005). Overall, there is little research done on the effect of shell shape on settlement rates, but it has been indicated that oysters prefer their shell's natural shape.

Biochemical cues.

Once the fertilized egg has developed through its life cycle into a pediveliger, it searches for a hard substance to settle upon and metamorphosize into a spat (University of Maryland Center for Environmental Science [UMCES]). This settlement stage and its location is often the most critical aspect of the oyster life cycle because this is where the spat develops into an adult oyster (UMCES). In the Chesapeake Bay, there is frequently a lack of settlement surfaces for the *C. virginica* pediverligers, interfering with the this crucial foundational step (Theuerkauf, Burke, & Lipcius, 2015). Oyster larvae have previously shown to preferentially settle and metamorphosize in response to environmental cues, usually associated with the substratum for settlement (Coon, Bonar, & Weiner, 1985). For instance, neuroactive

compounds, such as L-DOPA, GABA, serotonin, and acetylcholine, are frequently used to induce pediveliger settlement and metamorphosis (Grant, 2009).

Experiments with the pacific oyster, the eastern oyster, the flat oyster, and the tropical oyster have all shown that L-3,4-dihydroxyphenylalanine (L-DOPA) enhance larval settlement and metamorphosis (Teh, Zulfiger, & Tan, 2012; Mesias-Ginsbiller et al., 2013; Grant, 2009, & Coon et al., 1985). L-DOPA is an amino acid and a precursor to the neurotransmitter dopamine (Grant, 2009). Researchers have proposed two pathways to explain the effects of chemical cues on the oysters development: a dopaminergic behavioral pathway and an adrenergic morphogenetic pathway (Grant, 2009). L-DOPA is classified into the dopaminergic behavioral pathway because the environmental L-DOPA is converted to dopamine in the larvae and triggers substrate searching behaviors (Bonar, Coon, Walch, Weiner, & Fitt, 1990). While adrenergic precursors like epinephrine and norepinephrine induce metamorphosis, even without a settlement surface, L-DOPA encourages settlement and metamorphosis (Coon et al., 1985). According to experimental evidence, larvae settlement peaks at a L-DOPA concentration of 10^-4 M after 25 minutes (Grant, 2009; Beiras & Widdows, 1995; Coon et al., 1985; Walch,Weiner, Colwell, & Coon, 1999).

Materials and Methods

Questions and Hypotheses

3D printing possesses innate and unique qualities, including the possibility of efficient mass production, and the ability to use a filament with material appropriate for oyster restoration. We decided to employ this technology to assess whether its qualities might lend themselves to the production of a viable alternative substrate. As a result, the overarching question remained unchanged from Part One of the project:

How can artificial substrate be used to study methods of oyster restoration in the Chesapeake Bay? However, the team now had a more specific question to assess: Can additive manufacturing be used to study oyster settlement? This question guided the team's overall methodology for the remainder of the project. The team developed the following sub-questions:

1) Can 3D printing filament be used to create durable shells identical to natural oyster shells?

2) Do oysters settle and grow well on 3D printed substrate compared to the naturally occurring calcium carbonate substrate?

3) Can L-DOPA induce oyster settlement on 3D-printed shells?

To test these questions, we developed three hypotheses to direct the research. The first hypothesis guiding this project is that, using the resources available on campus, including the McKeldin Makerspace and Terrapin Works, we would be able to produce alternative shells that mimic the physical structure of natural oyster shells. This hypothesis would be evaluated by comparing similarities and differences between the printed shells and the natural shells. The second hypothesis is that oyster settlement and growth will not differ between naturally produced shells and printed shells. This would be assessed at the Horn Point Lab Oyster Hatchery, where spat settlement and growth rate could be measured and compared between the two types of shells. Finally, our third hypothesis was that L-DOPA would increase settlement rates on the printed shells. L-DOPA is an important chemical signal during natural oyster settlement, and studying its effect on settlement on the 3D printed shells could lend information about the role of chemical signals versus physical structure during settlement. In summary, our questions and hypotheses aimed to test the efficacy of 3D printed shells in order to better understand the relationship between chemical cues and

physical form of substrate during larval settlement and spat growth. The implications of this project could provide more insight into the role that 3D printing technology could have in restoration research.

Filament Choice

For the 3D printing process, we first looked for a printable filament that would also be suitable for fostering oyster settlement and growth. Given that oyster shells are composed primarily of $CaCO_3$, the team sought filament that contained a similar compound. The two filaments initially chosen were LAYBRICK and LAYCeramic, both of which are produced by Matter Hacks. The listed price of LAYBRICK is $144 for 1 kg, and the listed price for LAYCeramic is $200 for 1 kg. The team decided to use LAYBRICK since LAYCeramic was not described as containing calcium.The creators of LAYBRICK claim the filament contains “natural mineralic fillers” (super-fine milled chalk). For clarity, a team member also contacted the producers to find out more about its content. The team determined that LAYBRICK contained a notable amount of $CaCO_3$. As will be discussed later, LAYBRICK is also relatively brittle, which affects the printing process, and buoyant, which affects the Phase III methodology. We purchased five rolls in total, starting off with two at a time and buying more as supply ran low.

Filament Testing

After choosing LAYBRICK to print the artificial shells, we tested its physical reaction to prolonged exposure to saltwater. To model the 3D-printed oysters shells, we printed three 10.10x7.60x0.65 cm blocks consisting of about 22 g of LAYBRICK at 10% infill and tested buoyancy and water absorption. The blocks were submerged in a tank of water with a depth of 3 inches at 20^{o}C.

For the setup, Instant Ocean Mix was added to the tank to to resemble the environment of the Chesapeake Bay. A Goodes ATC Salinity reader measured the tank salinity at approximately 15 ppt, in the range of the Bay's brackish water (NOAA, 2017). Once the setup was complete, the three blocks were submerged in the tanks. Since the blocks floated in the saltwater, we placed 42 g metal diving weights on top of them to keep them underwater. We then measured the volume of water displaced with a ruler to get total brick volume and mass of water displacement. Afterwards, we calculated buoyancy by multiplying the mass of the water displaced times gravity (9.8 m/s^2). We used the change in mass of the blocks over time to quantify their water absorption. After 3 and 12 days, we recorded the mass, volume, and buoyancy of the blocks. Likewise, after 3, 12, and 38 days, we qualitatively observed the blocks for texture and strength changes.

3D Printing and Scanning

The natural shells to be scanned were obtained from Dr. Paynter's lab in the Biology-Psychology building of University of Maryland. These empty shells had been previously obtained from various sites in the Chesapeake Bay prior to the start of our project. The team subjectively selected shells, considering factors such as the curvature of the shell, light-reflective properties of any marks on the shell, any other notable features that would make meshing scans easier, and relative size of the shell to ensure it would fit on a scanner. In the end, the team selected approximately 20 shells that could subsequently be scanned, though not all were eventually scanned. Shells were picked to be scanned at random.

For the first two shells, the team used the Next Gen 3D Laser Scanner in the McKeldin Makerspace. Team members from Team WALK had previous experience with the available equipment at the space, and had an existing relationship with

Preston Tobery, on staff at the Makerspace. Scanning began on January 12, 2018 with one shell. For proper setup, the shell was secured by a rod on a plate such that it was in view of the scanner's camera (see Figure 26). Depending on the kind of scan, the plate would rotate in order to capture certain orientations of the shell, such as a a 360 degree scan, during which shell would rotate around. The team performed one 360 degree scan (i.e. the scanning platform rotated one revolution with the shell on it), then supplemented the results with single scans (i.e. the shell remained stationary) until all external surfaces were scanned. This typically required three to five single scans, depending on the surface geometry and reflectivity of the shell. After obtaining the images, the team used the scanner's software to remove unwanted data (such as noise or parts of the scanner) and mesh the images together as closely as possible. This process involves aligning analogous points on each scan so that they can be combined into one. Once this process was complete, the team extracted the scan file, leaving it ready to be printed.

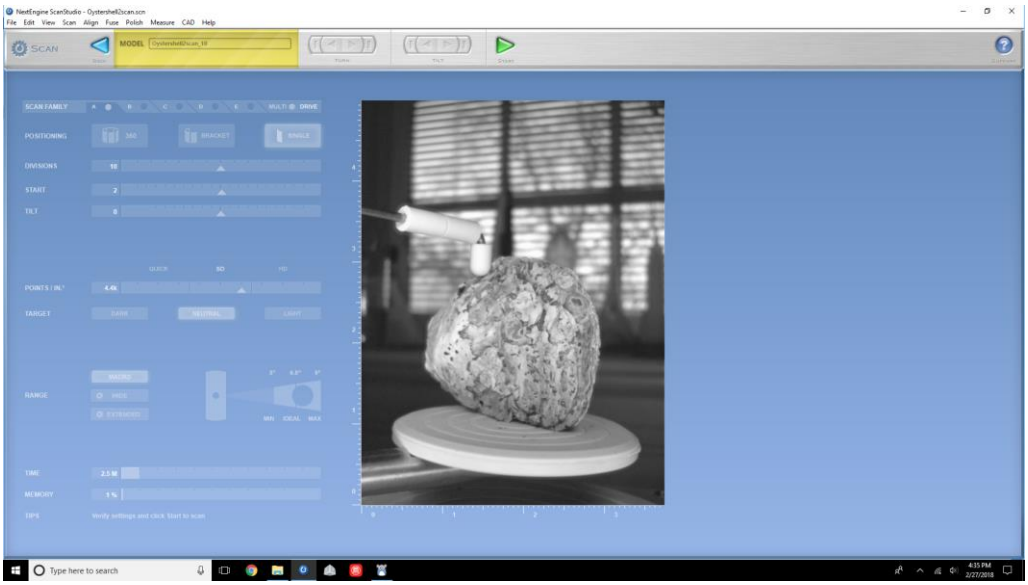

Figure 27: Screenshot of scanning process for a single shell

On the Next Gen scanner, the team scanned two shells by the middle of February. At this point, the team recognized that the scanning process was meticulous, required great attention to detail and time. To increase efficiency, the team transitioned to Terrapin Works, a student-run company that works with various additive manufacturing methods. As a result, the team was able to pay a student employee at Terrapin Works to scan 12 shells.

After a scan was completed, the team reviewed the file and ensured the scan was suitable for printing. This involved orienting the scan such that the shell was face-down, or having the concave side face the build plate. The team also made sure that the shell was as level as possible in order to minimize the amount of supports necessary for a successful print. Additional editing and supports were created via Meshmixer, resulting in a final scan that could then be sent to a printer for production.

Printing was conducted on Makerbot Replicator 2's, located at the McKeldin Makerspace and Terrapin Works. The team followed standard procedure for printing objects using Makerbots. First, the scan file was loaded into the Makerbot software. There were a few instances in which the printers were not connected to a computer, meaning that a print could not be initiated by a computer. In these situations, the team transferred the scan files onto SD cards, which then could be inserted into the printers directly. Given that the filament was prone to breaking, the team also took precautions to ensure that the print went smoothly. On occasion, the roll of filament would break. A team member would then manually stop the print and reload the filament into the extruder. Thus, there were usually one or two members present during every printing session for the shells. We used 10% diamond infill for each print. Printing time varied based on the volume of the shell and the amount of support material required to stabilize the print. The prints were typically performed with the inside of the shell

facing the build plate, as this was the most stable configuration and preserved the geometry on the more complex exterior of the shell. After the part was printed, team members manually removed the support material.

In total, nine shells were printed for the initial settlement testing phase. As will be discussed later, an additional 22 shells were printed for the second settlement testing phase in the

Fall. In the first phase, printing began in January of 2018, during the winter term, and was completed by April of that year. Shells, both printed and natural, were kept in sealed plastic bags until the team was ready to transfer them to the hatchery.

Settlement Testing Phase 1

We selected the Horn Point Oyster Hatchery as the site for the larval settlement experiments. The hatchery, located in Cambridge, Maryland on the Choptank River, produces oyster larvae for oyster restoration and research projects.The facilities enable the hatchery to carry out larval settlement in setting tanks. We chose the Horn Point Oyster Hatchery for its ability to produce and set oyster larvae as well as its location on the Chesapeake Bay, within driving distance of the University of Maryland.

In July 2018 the set of nine 3D printed shells and their natural counterparts were tested for settlement and growth at the hatchery. At the hatchery, all shells were attached to a mesh, cage-like structure that held them in place under the water . Each 3D printed shell was placed directly adjacent to its natural shell counterpart in order to eliminate the possibility that location in the mesh entrapment would impact the setting preferences of oyster larvae. Then, the mesh entrapment was placed into a 200 liter tank of seawater for 24 hours, which allowed the shells to acclimate to the seawater conditions. After the soaking period, the water was drained from the tank before being

re-filled with seawater. Then, *C. virginica* spat, provided by the hatchery, were subsequently introduced and left to settle on the shells for 48 hours. After 48 hours, 3D printed shells and natural shells were retrieved from the setting tanks for data collection. The number of spat on the artificial and natural shells were counted using a microscope, and recorded. On shells that had more than 50 spat, the count was reported as 50, in accordance with standard hatchery procedure. Then, the shells were placed back in the mesh entrapment and left in a tank of ambient water for 31 days to compare mortality rate of spat over time.

Settlement Testing Phase 2

After analyzing the results from the July 2018 setting experiment, we sought to further explore the impact of chemical and physical cues during larval settlement by carrying out another experiment at the hatchery. Results from the July experiment indicated that oyster larvae preferred to settle on the natural shells, which prompted a follow-up study to examine these results more in depth. We designed the following experiment to test whether a biochemical stimulant could enhance settlement on the 3D printed shells. The team selected L-3,4-dihydroxyphenylalanine (L-DOPA) to act as this stimulant based on existing studies that demonstrate its ability to enhance larval settlement (Teh et al., 2012, Mesias-Ginsbiller et al., 2013, Grant, 2009, & Coon et al., 1985). Thus, the overall purpose of this experiment was to test the presence of L-DOPA on 3D printed shells for improving larval settlement rates when compared to 3D printed shells not containing the biochemical stimulant.

In order to conduct this experiment, we required more 3D printed oyster shells before the end of the larvae production season. The team hired Preston Tobery at UMD's Makerspace to expedite the process and ensure the continuous oversight and production of the shells. Two sets of 11 3D shells (22 in total) were printed using the

saved scans from the previous experiment. We also gathered the equivalent amount of natural shells in order to compare settlement rates between natural and printed shells. As described in the hatchery methodology that follows, half of the shells would be set with L-DOPA while the other half would be set without L-DOPA. However, this time, each natural shell was not paired directly with a 3D printed shell; rather, the overall average of each group would be used to make the comparison.

Related studies that used this chemical to enhance oyster settlement support the concentration of 10^{-4} molar as the most effective level (Grant, 2009, Beiras & Widdows, 1995, Coon et al., 1990, Walch et al., 1999). Some studies, i.e. Grant, 2009, even show oyster larvae mortality at levels above 10^{-4}. Using this information, the team created a 10^{-4} molar stock solution of L-DOPA as this would allow for more equal mixing of the chemical into the setting tank. To make the stock solution in the lab, 3.94 g of L-DOPA were measured and mixed with about 500 mL of distilled water using a magnetic stir bar setup.

The stock concentration and oyster shells were then brought to the hatchery to begin the settlement testing. Many of the methods for this experiment were kept consistent with the previous settlement experiment at the hatchery, though new or revised methods were put in place as required by the differences between Phase 2 and Phase 1. This time, two separate tanks were filled with 200 liters of seawater. Again, the shells were left to soak in the seawater before creating the experimental conditions. After soaking for 24 hours, the water was drained. In the experimental tank, the stock solution of L-DOPA was added and allowed to distribute within the water, while the control tank was filled with 200 liters of regular seawater. All shells were evenly divided so that there were 11 3D printed shells and 11 natural oyster shells for each treatment. Then all shells were secured to a mesh entrapment (one for

each tank) and placed into their respective tanks for larval setting. In accordance with prior studies, the L-DOPA water was removed and replaced with regular seawater after 30 minutes of setting in order to avoid a toxic impact on the larvae (Grant, 2009). To do so, the water was drained and refilled as rapidly as possible to avoid disturbing settlement. After 24 hours, all shells were removed from the tanks for data collection, at which time the number of spat on each shell was counted and recorded.

Results

LAYBRICK Testing

Before introducing the LAYBRICK filament to live oyster larvae, we examined its physical properties as a solid, printed object. Three 3D-printed blocks were submerged in artificial seawater for 38 days. Table 1 outlines the averaged results of the three LAYBRICK-printed blocks.

The blocks absorbed an average of 4.5 g of water after three days and 7.3 g of water after twelve days. The volume and buoyancy of the shells did not change, implying that the water was in the hollow infill space rather than the filament itself. After three and twelve days, the blocks remained intact and rigid to the touch.

After 38 days in the saltwater, the blocks remained intact without pressure. However, with light pressure, the blocks felt weak and were easily broken. Water had evaporated from the tank, so the blocks were left in highly salinated water which could have contributed to the brittleness. We did not collect mass and volume measurements on day 38 because of the brittle nature of the blocks. Overall, we concluded that the LAYBRICK filament was sufficiently strong for spat settlement in the short-term context of this experiment, but may not be viable for long-term deployment in seawater.

Table 1: Physical property results of LAYBRICK-printed blocks in salt water			
Average of Three Blocks	Day 0	Day 3	Day 12
Mass (g)	21.9	26.4	29.2
Volume (cm^3)	46.61	46.61	46.61
Buoyancy (N)	0.3514	0.3514	0.3514
Qualitative Observations	Blocks were stiff and intact	Blocks remained structurally sound when light pressure was applied	Blocks remained structurally sound when light pressure was applied

Settlement Testing

Before discussing our results, we must first discuss how the data are reported. Standard procedure at Horn Point Hatchery is to count all of the spat up to 50. At or above 50 spat, the count is reported as 50. In other words, 50 serves as a threshold value, and at that point, the shell can be considered "fully populated", for our purposes. We can therefore present the data as each shell's spat count relative to the threshold. For example, a spat count of 50 is 100% of the threshold, and a spat count of 25 is 50% of the threshold. Throughout our presentation of the results, we will first report the mean spat count for each category of shells, in order to as we did when analyzing the data, and then report the spat count as a percentage of the threshold value.

Phase 1.

The first set of settlement data was collected over the summer. In total, we tested 18 shells, nine of which were printed shells and nine of which were natural. This session of spat settlement was assessed two different dates: July 27, 2018, and

August 28, 2018. The specific counts for the two groups sorted by date are reported in Tables 2 and 3. The difference over time is displayed in Table 4. The mean spat count of the natural shell group on July 27 was 50. The mean spat count of the 3D-printed group on July 27 was comparatively smaller (M = 5.444, SD = 3.321). Thus, at first glance, there is a stark difference between the two groups. By August 28, the natural shells (M = 45.556, SD = 13.333) had clearly outperformed the printed (M = 0.444, SD = 0.527). We do not know why Natural Shell No. 2 lost 40 spat from July to August, altering the mean and standard deviation, but theorize that may have been due to issues outside of our control. This may have resulted from problems with the shell itself, for example, such as substantial brittleness deforming the shell. We consider this shell to be a statistical outlier due to the fact that the other shells retained their spat, and Natural Shell No. 2's analytical inclusion drastically increases the standard deviation. We discuss this in more depth shortly in our discussion of the difference within pairs in spat count. When Natural Shell No. 2 is excluded, the average is again 50. Overall, the average for all shells on July 27 was slightly higher was (M = 27.722, SD = 23.037) than the average for August 28 (M = 23.000, SD = 24.949).

Table 2: July 27, 2018					
Natural			Printed		
Tag Number	Shell Number	Spat Count	Tag Number	Shell Number	Spat Count
1	1	50	1	1	1
1	2	50	1	2	9
1	3	50	2	3	1
2	4	50	2	4	7
3	5	50	3	5	9
3	6	50	3	6	8
3	7	50	3	7	5
4	8	50	4	8	7
4	9	50	*	9	2

*The tag number for this shell was lost.

Table 3: August 28, 2018					
Natural			Printed		
Tag Number	Shell Number	Spat Count	Tag Number	Shell Number	Spat Count
1	1	50	1	1	0
1	2	50	1	2	1
1	3	50	2	3	1
2	4	10	2	4	0
3	5	50	3	5	1
3	6	50	3	6	0
3	7	50	3	7	0
4	8	50	4	8	1
4	9	50	0**	9**	0**

** The data for Shell No. 9 was lost. For analytical purposes, such as the average of printed shells on August 28, the count was assumed to be zero.

Table 4: Summer 2018 Over Time; Printed Shells			
Tag Number	Shell Number	Spat Count (7/27)	Spat Count (8/28)
1	1	1	0
1	2	9	1
2	3	1	1
2	4	7	0
3	5	9	1
3	6	8	0
3	7	5	0
4	8	7	1
4	9	2	0

To assess the difference between the printed group and the natural group, the team employed the Wilcoxon Signed Rank Test, which is suitable for testing the difference between two populations in paired studies with small sample sizes, provided that the data is ordinal or continuous. To perform the test, the team also assumed that the difference between the two populations is symmetrically distributed. This cannot be confirmed, as the actual number of spat on each shell exceeded the recorded value if there were more than 50 spat on the shell. For July 27, we

discovered that there was an observable significant difference between the natural and printed groups (t = 122.912, p < 0.01) (SD = 16.882). On average, the printed and natural pairs differed in spat count by 44.555 spat, meaning that the natural shells generally had about 45 more spat than their printed counterpart (SD = 3.321). For August 28, there was again a significant difference in spat settlement between the two groups (t = 130.080, p < 0.01) (SD = 16.882). On average, the printed and natural shells differed by 44.5 spat, which is not a substantial difference from the July testing (SD = 13.949). However, we believe that this average includes an outlier in Natural Shell No. 2, which increased the standard deviation. Thus, when this outlier is removed, the difference between the two pairs is more readily apparent (M = 49.429, SD = 0.535). Given that the difference is larger, this average indicates that the natural shells retained more of their spat, further demonstrating the difference between natural and printed shells. As a result, for analytical purposes, we include Natural Shell No. 2, as noted in the previously reported Wilcoxon Test results. However, for data presentation purposes, namely graphs and figures, we exclude the outlier to show the stark difference between natural and printed shells, as seen in Figure 31. Finally, the team also assessed the spat change over time. It is typical for later estimates to exceed initial counts, as freshly settled larvae are too small to count. However, the number of spat present on the printed shells declined significantly, suggesting that the artificial substrate does not provide adequate conditions for oyster settlement (t = 17.293, p < 0.01) (SD = 14.283).

The differences both over time and between printed and natural shells with respect to each group's means are graphically represented in Figures 28, 29, 30, and 32. Figure 31 in particular shows the paired comparison of spat count, showing the average difference between the natural shell and its printed counterpart on both dates.

Natural Shell No. 2 is excluded from the data for presentation purposes. As previously mentioned, we can also consider the spat count as a percentage of the threshold value (50 spat). This data is presented in Figures 32, 33, and 34. Threshold percentages were calculated by first finding the average spat count, as previously described. This value was then divided by 50 and subsequently multiplied by 100%, giving the percentage of the threshold. Figures 32, 33, and 34 demonstrate how natural shells met the threshold, while printed shells did not. Furthermore, printed shells did worse with respect to the threshold over time, showing their lack of ability to retain spat.

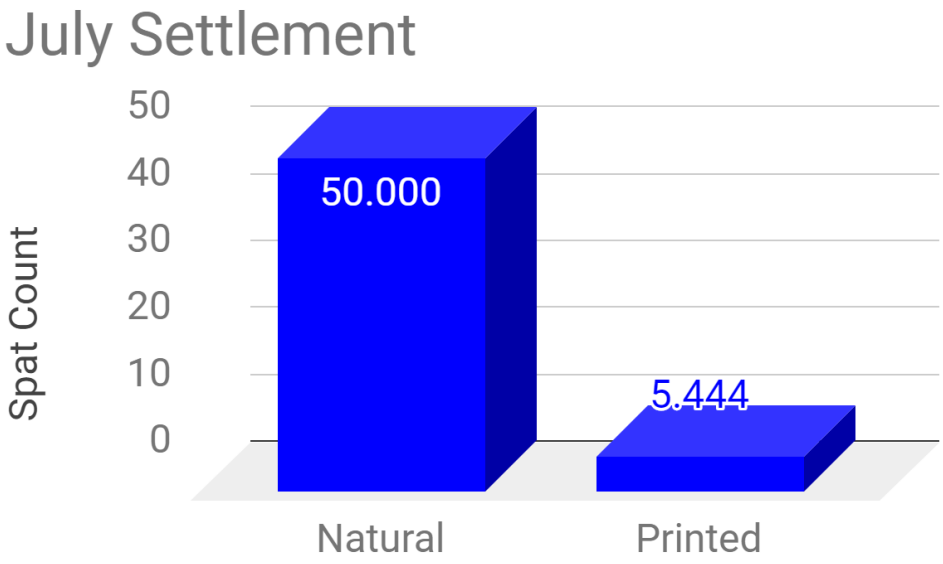

Figure 28: Natural and printed shells on July 27, 2018

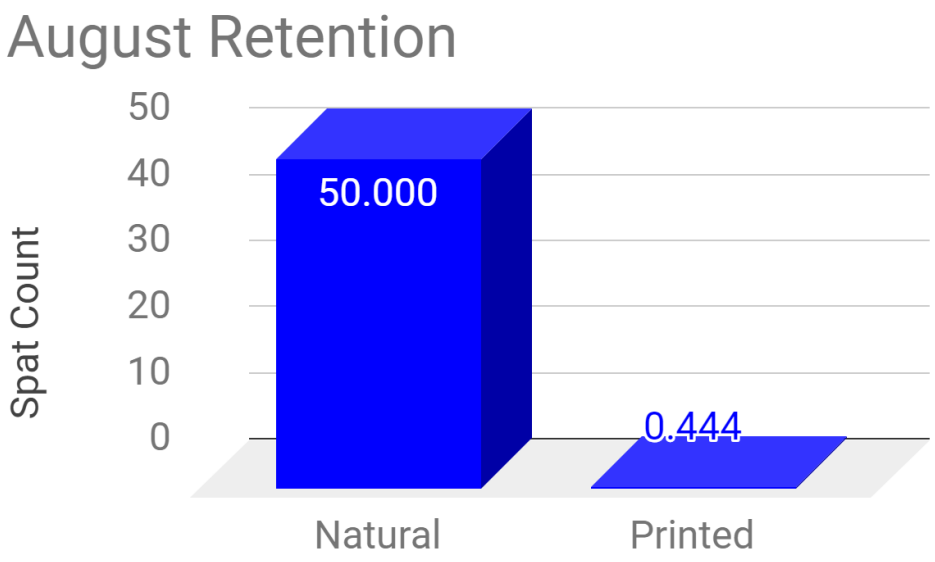

Figure 29: Natural and printed shells on August 28, 2018

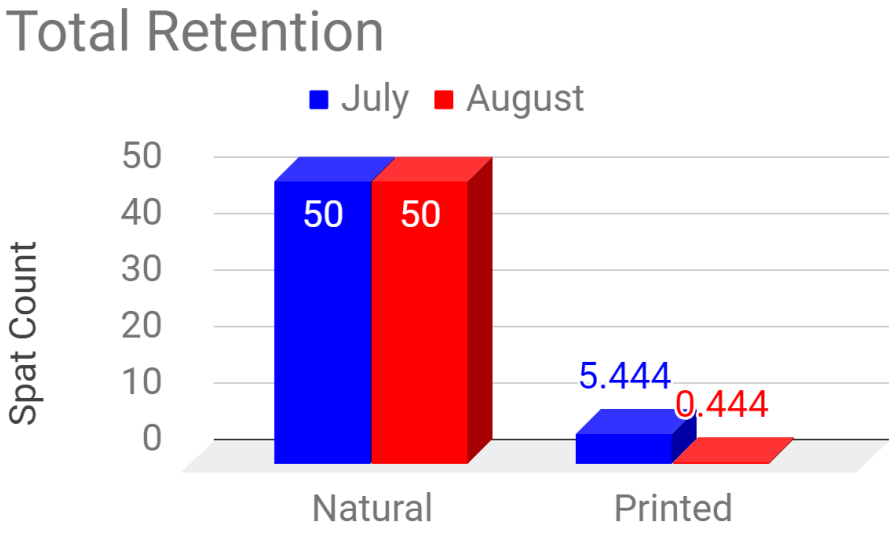

Figure 30: Shells over time

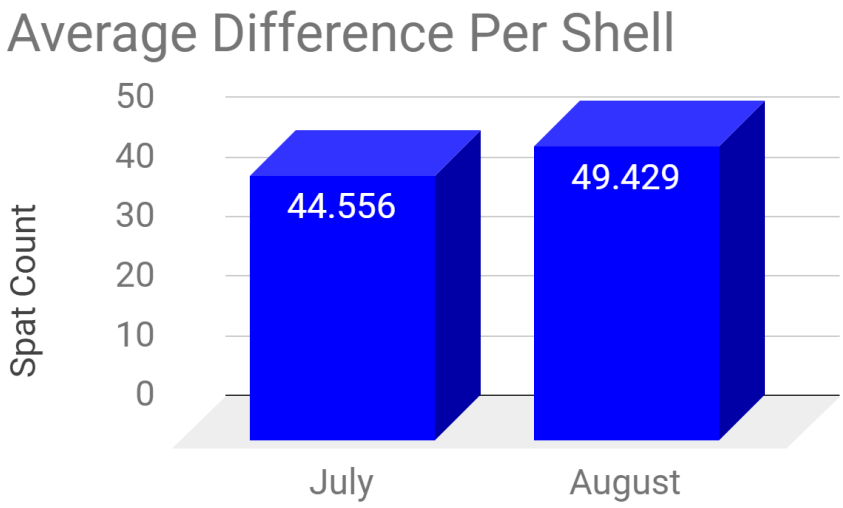

Figure 31: Difference within pairs in spat count

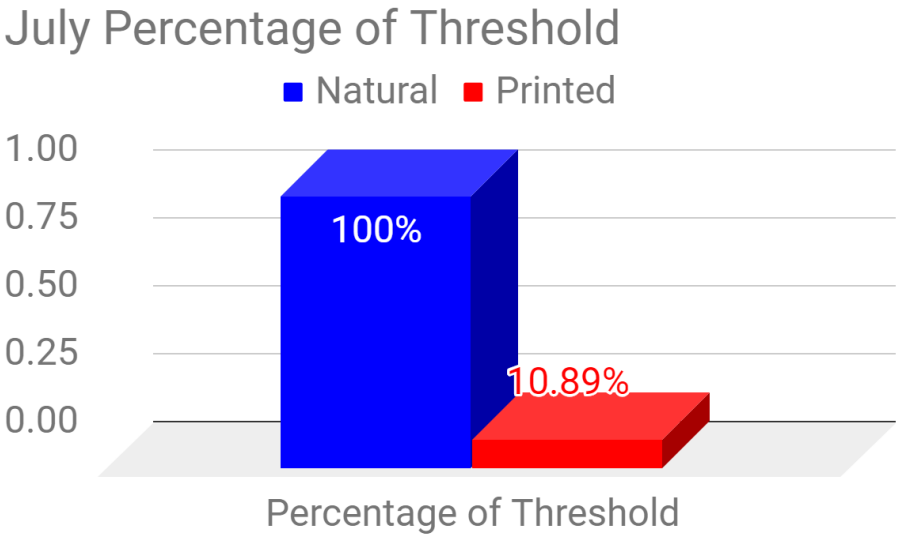

Figure 32: A comparison of July natural and printed shells with respect to threshold

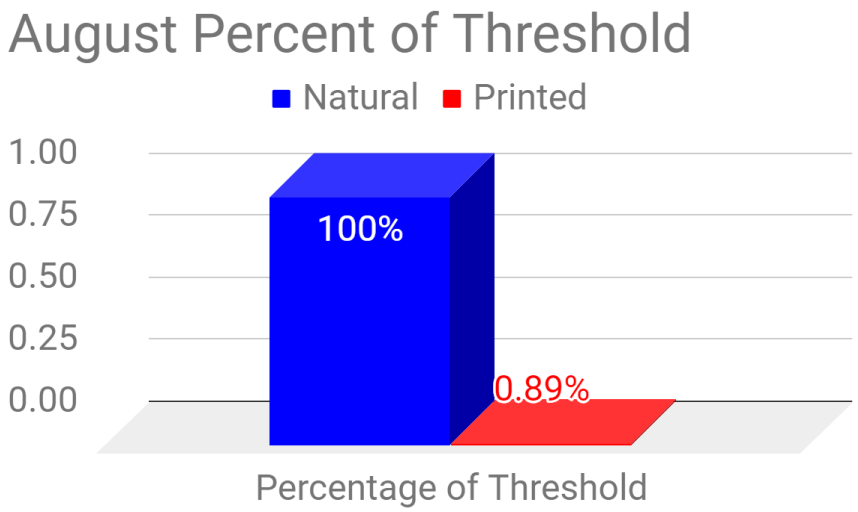

Figure 33: A comparison of August natural and printed shells with respect to threshold

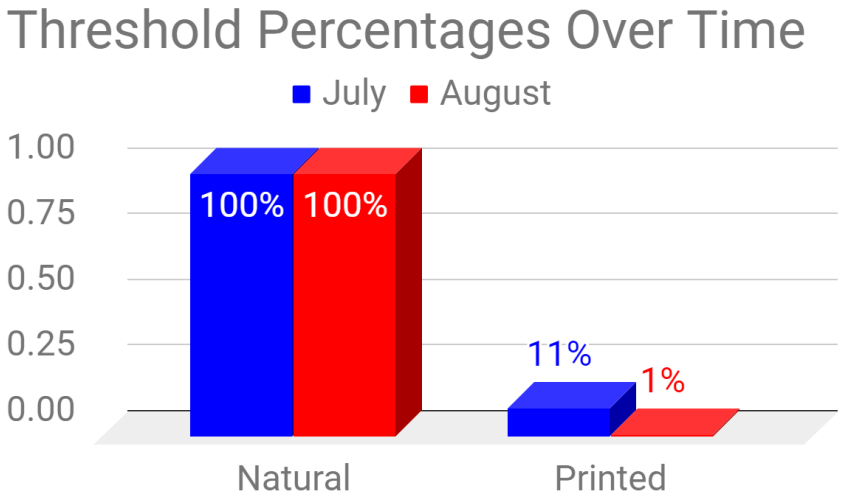

Figure 34: Percentages over time

Phase 2.

The results for all shells from the second settlement testing phase differed from the first upon primary glance (M = 5.182, SD = 10.669). This experiment was conducted following a hurricane, which can affect the water salinity and pH and may help explain why there were fewer spat overall. Additionally, the experiment occurred toward the end of the spawning season, so larvae may have been less robust than those used in the previous experiment. As described in the methodology, we

employed four distinct conditions: (1) Natural shells in control conditions, (2) 3D shells in control conditions, (3) Natural shells in L-DOPA conditions, and (4) 3D shells in L-DOPA conditions. The spat count means corresponding to each condition are presented in Table 5. We also computed the means for all shells in each of the four groups, meaning all natural shells, all printed shells, all L-DOPA tank shells, and all control tank shells, so there was overlap in the means. This would later be used in the ANOVA analyses. There were more spat on control tank shells (M = 8.545, SD = 14.064) compared to L-DOPA tank shells (M = 1.818, SD = 3.404), and there were more spat on natural shells (M = 9.682, SD = 13.740) compared to printed shells (M = 0.682, SD = 1.359).

Table 5: Comparison of Means across Conditions

Means	Natural Shells	Printed Shells
L-DOPA Tank	2.818	0.818
Control Tank	16.545	0.545

Natural shells in the L-DOPA (M = 2.818, SD = 4.535) had more spat than printed shells in the same tank (M = 0.818, SD = 1.250). It should be noted that Natural Shell No. 2 had significantly more spat that the other shells, indicating that it may be a statistical outlier. Overall, the spat count for shells in the L-DOPA tank were much lower than anticipated. Natural shells in the control tank (M = 16.545, SD = 16.501) also outperformed printed shells in the same tank (M = 0.545, SD = 1.508). There was a high amount of variance in the natural condition, though it is clear that

the natural control shells had more spat than the L-DOPA shells. Spat counts are reported in full in Tables 6 and 7.

Table 6: September 24, 2018, L-DOPA Condition			
Natural		*Printed*	
Shell Number	Spat Count	Shell Number	Spat Count
2	15	1	0
5	7	3	0
8	2	4	1
10	0	9	0
12	1	11	2
14	0	13	0
15	3	16	4
19	1	17	0
22	0	18	1
23	2	20	1
24	0	21	0

Table 7: September 24, 2018, Control Condition			
Natural		*Printed*	
Shell Number	Spat Count	Shell Number	Spat Count
3	8	1	0
5	50	2	0
7	9	4	1
9	19	6	0
10	2	8	0
11	3	12	0
14	13	13	0
15	18	17	0
16	1	18	0
19	14	20	0
21	45	22	5

We analyzed the data using independent samples t-tests, correlations, and an univariate general linear model, or ANOVA. All analyses were done in SPSS. Most notably, we assessed the relationship between the printed shells and natural shells in the L-DOPA condition to understand whether L-DOPA decreased the divide in terms of spat count between the two kinds of shells. There was not a significant relationship

between the printed shell mean and the natural shell mean in the L-DOPA tank, indicating that L-DOPA did not contribute to a significant difference between the two shell types (t = 1.410, p = 0.174). Similarly, amongst the printed shells, there was not a significant difference between the means of the shells in the L-DOPA tank and the shells in the control tank, meaning that L-DOPA did not change spat settlement for printed shells (t = -0.462, p = 0.649). However, in the control tank, we did observe a significant difference between the means of the natural shells and the printed shells (t = 3.203, $p < 0.01$), and amongst natural shells, there was a significant difference between the means of the shells in the L-DOPA tank and the shells in the control tank (t = 2.661, p = 0.015). These statistics indicate that first, the natural shells again outperformed the printed shells, and second, that L-DOPA actually limited spat settlement on natural shells.

We used correlations to assess the relationships between the four conditions. The relationship between the natural L-DOPA shells and the natural control shells was weak and insignificant (r = 0.083, p = 0.808). The relationship between the natural L-DOPA shells and the printed L-DOPA shells was also weak and insignificant (r = -0.130, p = 0.704). The relationship between the printed L-DOPA shells and the printed control shells was the same (r = -0.207, p = 0.541). However, the relationship between printed and natural shells in the control tank was marginally significant, and moderate (r = 0.542, p = 0.085). The final two correlations were not as relevant to our analyses and conclusions, and are reported alongside the previous ones in Table 8.

Table 8: Correlation Matrix for the Four Conditions					
		Printed L-DOPA	Printed Control	Natural L-DOPA	Natural Control
Printed L-DOPA					
	Pearson's Correlation	1	-0.207	-0.13	-0.334
	Significance		0.541	0.704	0.315
Printed Control					
	Pearson's Correlation		1	-0.218	0.542
	Significance			0.519	0.085
Natural L-DOPA					
	Pearson's Correlation			1	0.083
	Significance				0.808
Natural Control					
	Pearson's Correlation				1
	Significance				

Finally, we employed a two-factor ANOVA to assess the main effects of the two independent variables of tank setting and shell type and the interaction effect between the two independent variables on the dependent variable of spat count. The main effect statistic in ANOVA assesses whether an independent variable had a significant effect on the outcome of the dependent variable, while the interaction statistic assesses whether the effects of one independent variables changes based on the presence of another independent variable. We found a statistically significant interaction between the effects of the independent variables on the dependent variable ($F(1, 40) = 7.267$, $p = 0.01$). In other words, for the natural shells, the L-DOPA tank seemed to decrease spat count, while for printed shells, the L-DOPA tank slightly increased spat count. L-DOPA had differing effects depending on the shell type. The main effect of tank setting was significant, as shells in the control tank had more spat than shells in the L-DOPA tank ($F(1, 40) = 6.712$, $p = 0.013$). The main effect of shell type was also significant, as natural shells had more spat than the printed shells ($F(1, 40) = 12.013$, $p < 0.01$). The corresponding partial Eta Squared values were 0.144 and 0.231, indicating that both had significant effects, and that the effect of shell was noticeably stronger. In summary, the combination of printed shells and L-DOPA as a chemical cue did not produce the expected significant increase in spat count.

The average spat counts for the respective conditions are graphically compared in Figure 35, 36, and 37. In addition, we again employed the threshold percentage statistic to understand in depth how the shells compared to each other, as seen in Figures 38, 39, and 40. The percentages again highlight the deficits created by using printed shells. The percentage values also show the differences between Phase 1 and Phase 2, in that only one shell (a natural shell in the control tank) reached threshold values. This idea is discussed further in the following section.

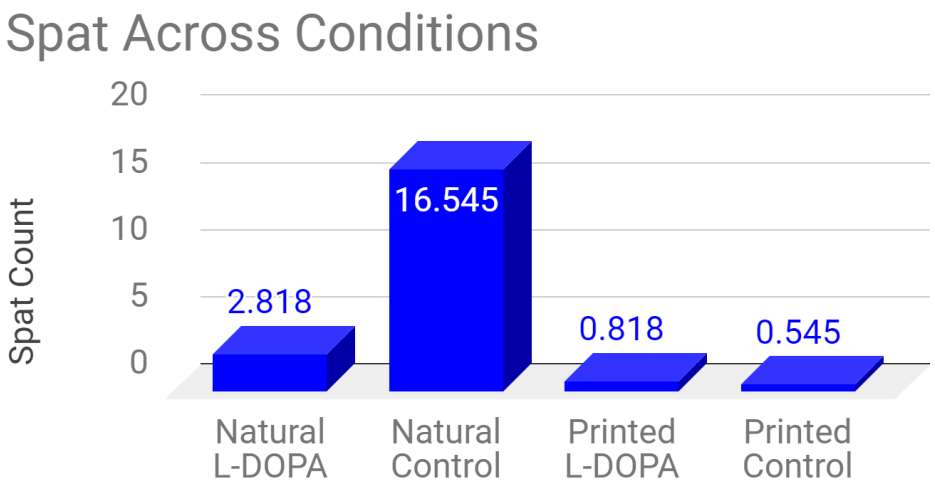

Figure 35: Spat count across conditions

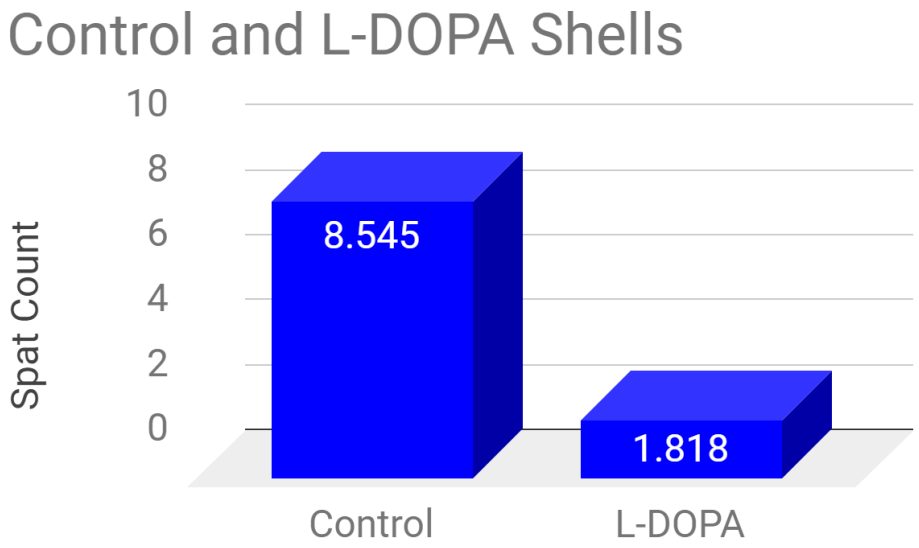

Figure 36: Spat Count between control and L-DOPA tanks

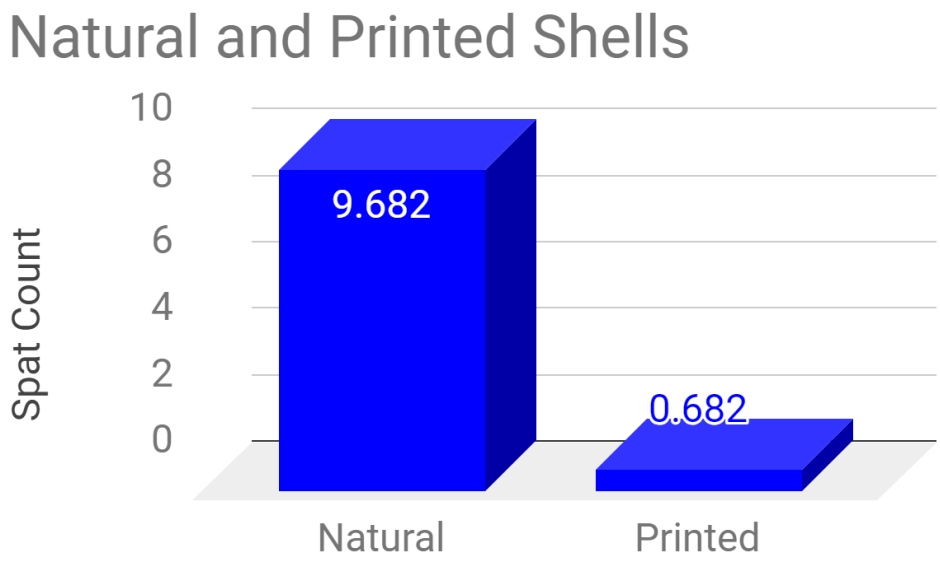

Figure 37: Spat count between natural and printed shells

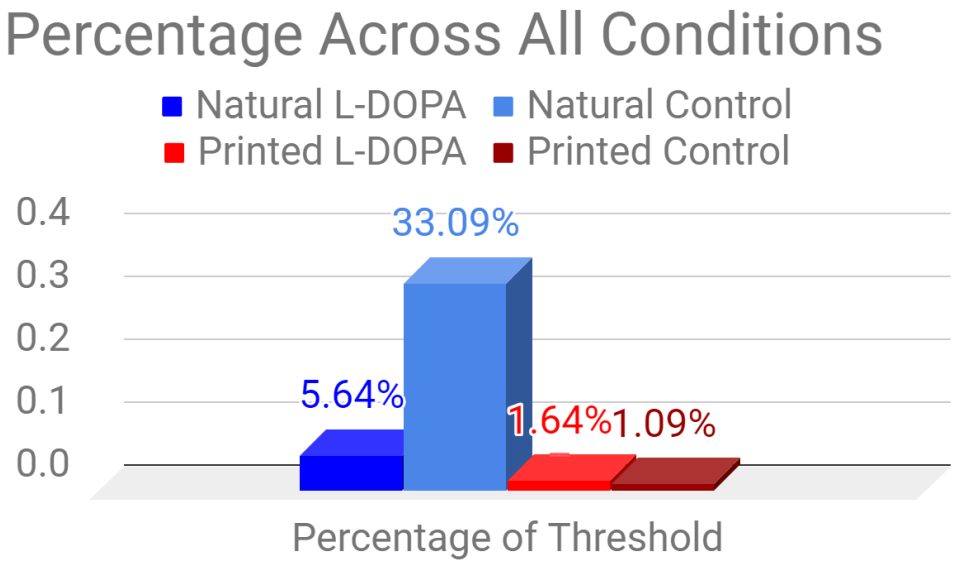

Figure 38: Percentage comparisons for all shells

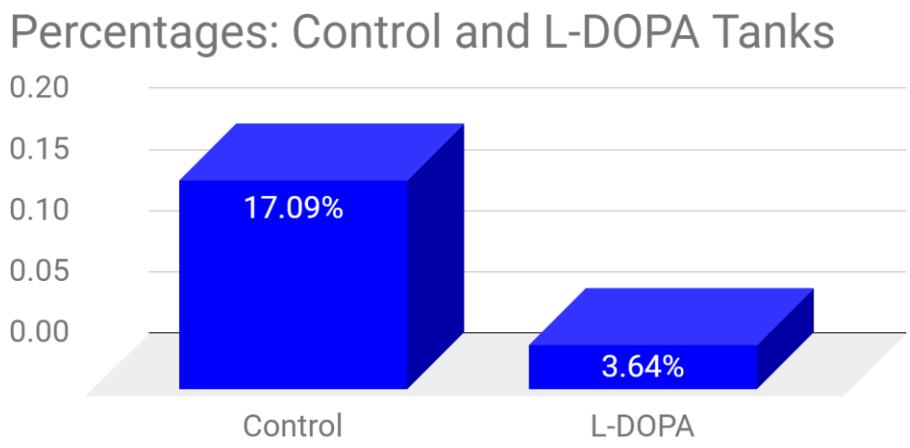

Figure 39: Percentage comparisons for control and L-DOPA tanks

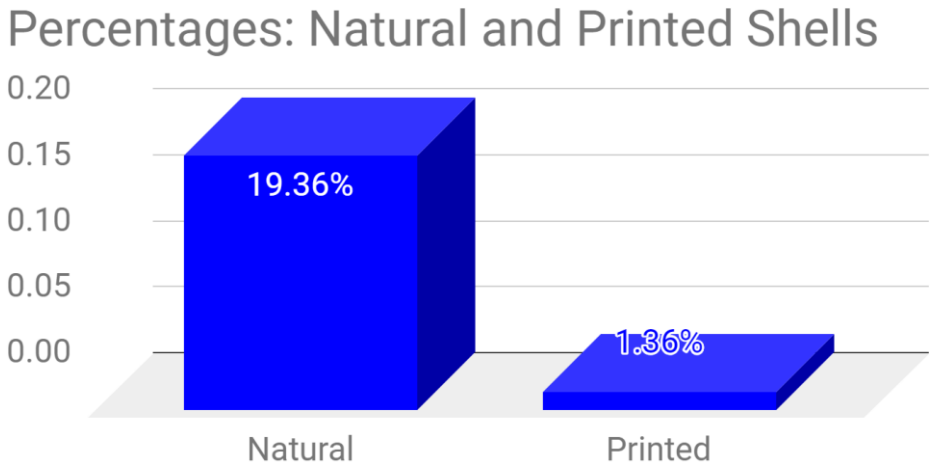

Figure 40: Percentage comparisons for natural and printed shells

Discussion

LAYBRICK Testing

The LAYBRICK filament testing was an extremely important assay to begin our examination of additive manufacturing in an aquatic setting. Few researchers have used 3D printed objects in a marine environment; therefore, we had no information on LAYBRICK's utility submerged in water.

One important discovery from the LAYBRICK testing was the high buoyancy of the test blocks. Throughout the twelve days of the testing, the average buoyancy

remained 0.3514 N. Unlike natural oyster shells, the test blocks floated in the tanks. In this case, we used small diving weights to submerge the blocks. Looking forward to our next step, we decided to use wires to hold the artificial shells to the underwater structure during settlement testing.

While the test blocks gain mass over time, their volumes and rigidity all remained consistent. This eliminated the concern of the artificial oyster shells absorbing water and becoming soft and spongy. Based on our data, we concluded that the LAYBRICK filament was sufficiently strong for spat settlement in the short-term context of this experiment. After this conclusion, we then proceeded to print oyster shell replicas using LAYBRICK for the purpose of spat settlement in a saltwater tank.

Settlement Testing

In the end, we did not observe significant settlement rates in either phase of settlement testing for printed shells. Comparing the averages for the two phases, we see that there was significantly more settlement on all shells for both summer dates (M = 27.722, SD = 23.037*)* *(*M = 23.000, SD = 24.949) in comparison to the fall date (M = 5.182, SD = 10.669) (see Figure 41). Similarly, as previously discussed, only one of forty-four shells reached threshold values in September, while all natural shells did in the summer. It is important to note when examining these differences that a direct comparison can only be made between the July date and the September date, as both assessed spat count within 48 hours of larvae exposure. However, based on the results over the summer, it is reasonable to predict low survival rates if testing had continued in September. As referenced earlier, the fall date was during a hurricane, which could affect oyster growth and settlement rates. Furthermore, the fall date was also towards the end of the hatchery's season, particularly as the water cooled down,

making it less suitable for inducing settlement. These two theories are discussed in further detail at the end of this section, alongside other limitations.

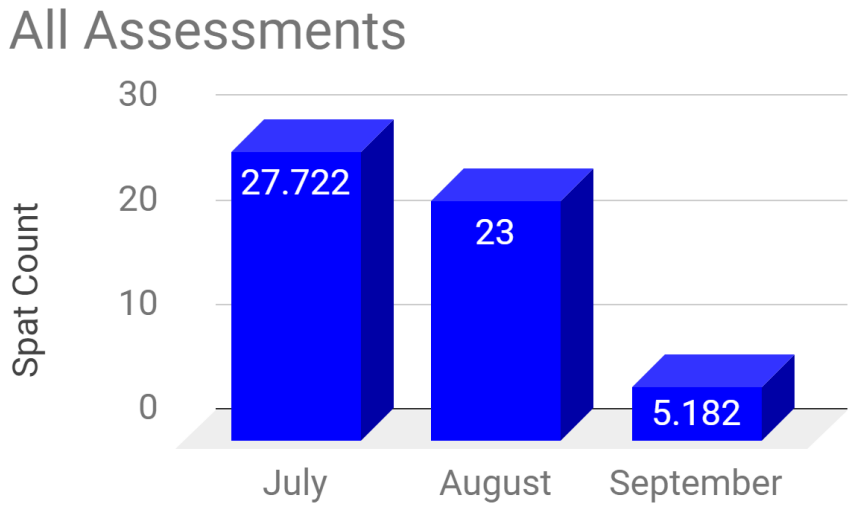

Figure 41: Average spat count per date

However, our overall hypotheses that the printed shells would be suitable for spat settlement could not be supported. In the summer, we found that the printed shells were significantly less effective at settling spat. This was true both in terms of initial counting, and particularly in the case of survival over time, as we observed that the printed shells lost oyster spat over time. By comparison, the natural shells maintained their spat count over the next month, as expected, save for the outlier of Natural Shell No. 2. Thus, the printed shells did not meet the standard set by the natural shells. We suspect that the chemical composition of the printed shells, which contained plastics dissuaded oyster larvae from settling on the material, despite its calcium carbonate content. The plastics in printed shell were form the filament LAYBRICK's plasticizers and copolyesters, which allowed the material to be malleable and meltable for printing. The plastics in the shells may have been noxious to the organisms, making them averse to settling. Furthermore, the results also indicate that the physical similarity of the printed shells to the natural shells was not

important in inducing settling behavior. The printed shells were duplicates of the naturals, and yet, were not suitable for settlement. Given this fact, and the hypothesis that the plastic components of the shells were toxic to the larvae, we conclude that the chemical composition of settlement substrate is of utmost importance relative to the geometric composition.

Given this working conclusion, we decided to test this principle by including chemical cues, namely L-DOPA. Based on existing literature, L-DOPA is theorized to promote settlement behavior, making it a prime candidate to induce behavior on the printed material. Specifically, we predicted that the L-DOPA conditions would have more spat than their control counterparts, and that the L-DOPA printed condition would have settlement rates on par with a natural setting condition. However, these hypotheses were not supported. First, we saw that L-DOPA seemingly made it less likely for spat to settle. While the average number of spat on printed shells in the L-DOPA tank was slightly, and insignificantly, higher than those in the control tank, the opposite was true at a significant level for natural shells. In other words, the presence of L-DOPA seemingly made it less likely for spat to settle on the natural shells. This could indicate that our choice of settlement cue was not effective in inducing settlement. In the literature, while L-DOPA has been seen to induce settlement, there is also some research that indicates that it may be slightly toxic, especially at higher doses (Grant, 2009). While in opposition to our hypothesis, the results may lend support to this idea.

Second, we saw that the printed L-DOPA shells did not perform as expected. We expected that the printed L-DOPA shells would have settlement rates on par with natural control shells, while this was not supported by the results. In short, this finding suggests that even with the presence of a biochemical settlement cue, the plastics in

the filament may restrict the printed material from being viable in oyster restoration efforts and research. Further, we also have additional evidence to support the claim that chemical viability overrides geometric similarity, to the point that settlement cues cannot eradicate this effect.

It is important to note the subtle differences in our methodology for the two phases of settlement testing, which in turn affected our analyses. In the first phase, we were interested not only in the differences between the two kinds of shells, but also change over time. Change over 31 days allowed us to determine whether oyster growth rate was affected by the printed shells. Alternatively, in the second phase, we were only interested in settlement rates, as that would tell us whether L-DOPA had a meaningful effect. Thus, we were not interested in growth over time. As such, our analyses for the first phase, employing Wilcoxon Signed Rank Test, accounted for changes over time, while our analyses for the second, primarily employing an ANOVA, did not.

There are several possible limitations for our experiment. The most notable is our relatively low sample size. We were only able to print nine shells for the first round of settlement testing. The first scanner we used was relatively slow, limiting our ability to scan multiple shells. We were also delayed by having to initially edit the scans ourselves, which we were only able to complete whenever a team member was free. We eventually transitioned to another scanner, staffed by a Terrapin Works employee, allowing us to speed up the process. Having a smaller sample for both phases could limit the power of our study, as it could be that the results would paint a different picture with a larger sample. However, the relevant results, as indicated by our research questions, clearly and significantly indicated that the printed shells were at a disadvantage relative to natural shells.

A second limitation is that for the first batch of nine printed shells, the process of scanning and printing differed. We initially used the resources in the Makerspace before using Terrapin Works. In theory, this could mean that some shells had more detail than others. While microclimate effects can be powerful, we believe that any differences would be negligible, as all printed shells replicated natural shells. Third, we used different printers depending on what was available for the first nine printed shells, either in Terrapin Works or the Makerspace. However, again, any differences should be minimized that the printers were all Makerbot Replicator 2's. This variance was accounted for in the second settlement testing phase, as all twenty two shells were printed in the Makerspace.

A fourth possible limitation was the effects of a recent hurricane, which could have affected the second phase of settlement phase. For example, temperature changes, such as those associated with hurricanes, have been seen to negatively affect oyster growth (Speights, Silliman, & McCoy, 2017). However, since experiments are typically done in tanks, standard procedure during hurricanes at the Horn Point Hatchery is to adjust salinity levels to make the conditions as naturalistic as possible. Data from the hatchery indicates that many aspects of the water quality were similar between the two settlement dates. For the July phase, the pH level was 7.69, the temperature was 27 degrees Celsius, and the salinity level was 9.7, while for the September the corresponding values were 7.45, 29.3, and 9.8. Thus, these values were essentially consistent throughout testing.

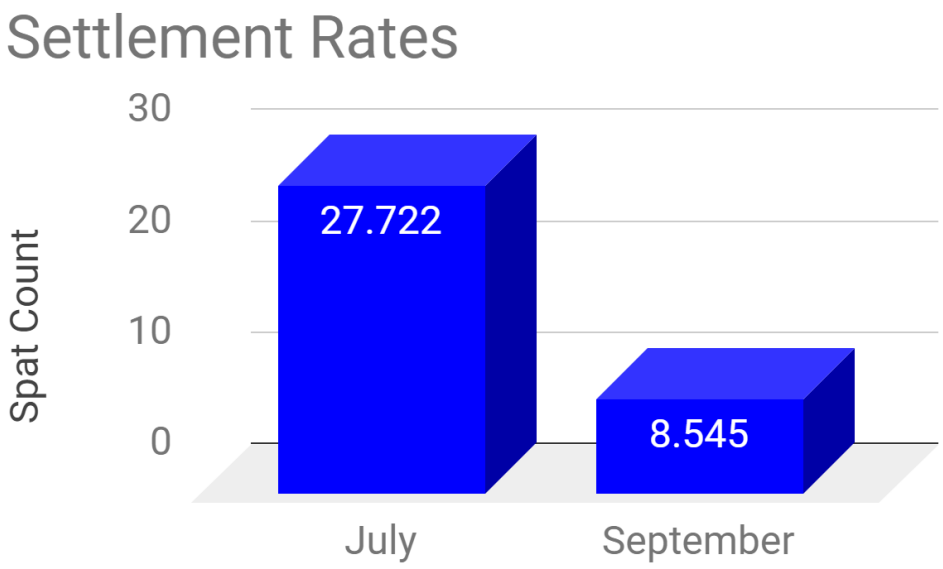

Figure 42: July mean and adjusted September mean

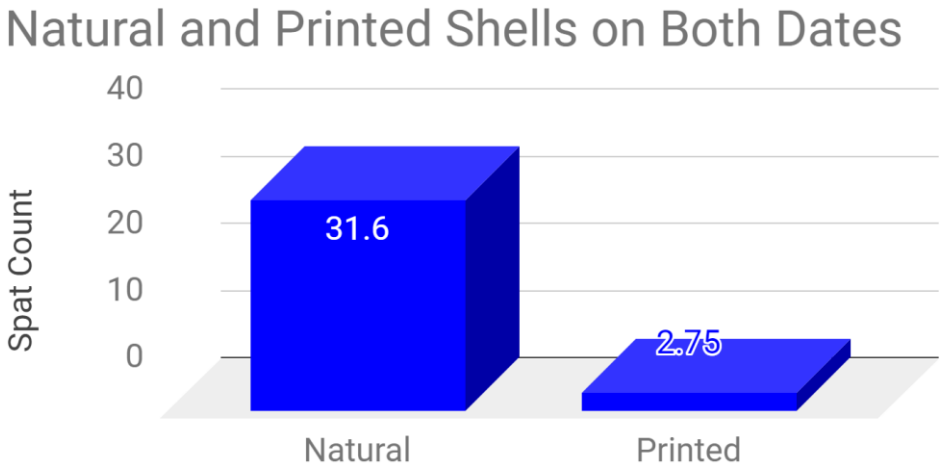

Figure 43: Natural and printed means for both phases

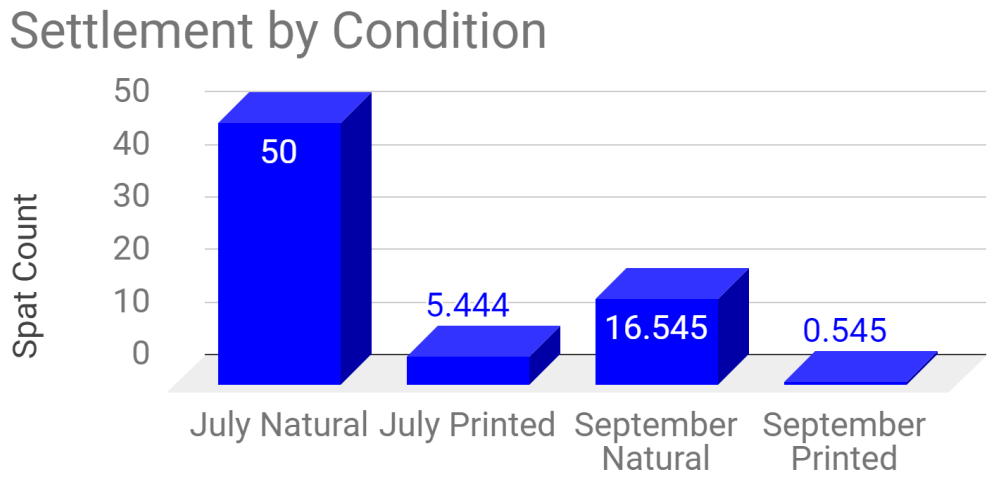

Figure 44: Date by Shell Means

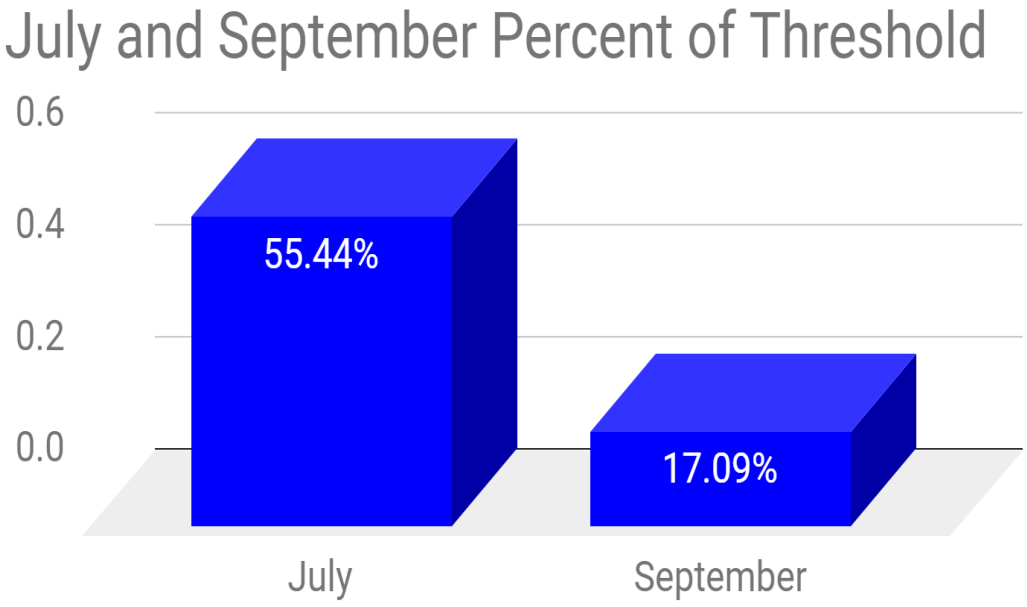

Figure 45: Percent of threshold between phases

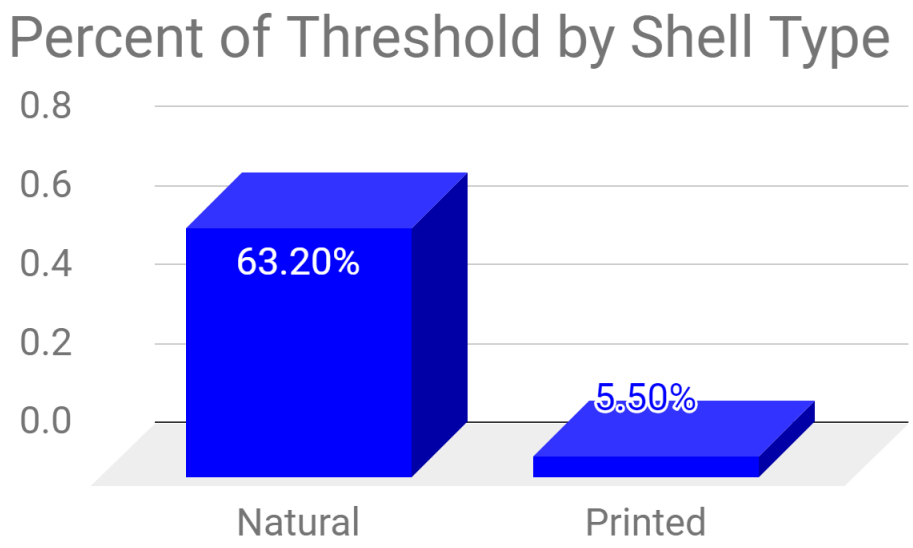

Figure 46: Percent of threshold divided by type of shell including both phases

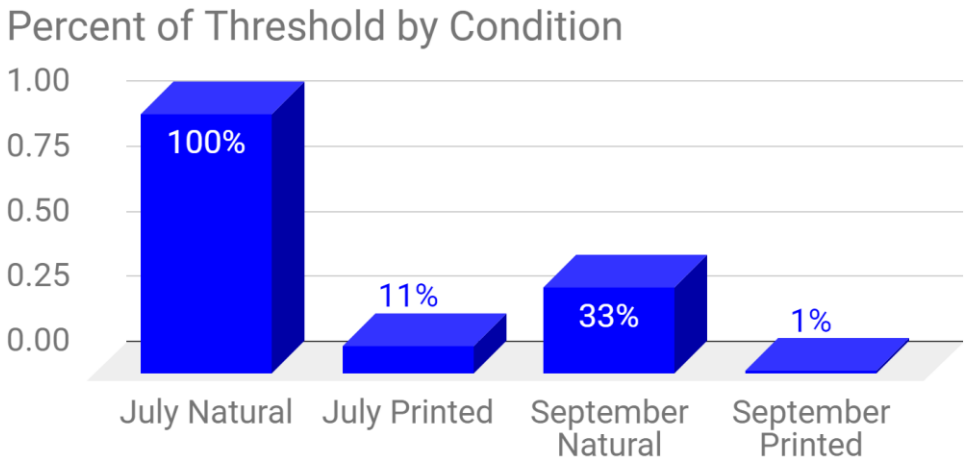

Figure 47: Percent of threshold divided into the four conditions

To analyze if the hurricane might have possibly had an effect, we compared the spat count for all shells in the July session to the spat count of all shells in the control tank of the September session. Figures 42, 43, and 44 detail how natural shells outperformed printed shells across both dates by comparing various spat count averages, while Figures 45, 46, and 47 do the same using percentage of threshold. As detailed in Table 9, shell type still contributed to significant differences in spat count when incorporating the data from both dates, as evidenced by a one-way ANOVA

($F(1, 38) = 37.242$, $p < 0.01$). The partial Eta Squared corresponding to this statistic was 0.495, indicating a clear and strong impact of differences in shell type. When the differences between the conditions associated with the two dates (pH, salinity, temperature) are taken into account as an additional variable by conducting a two-way ANOVA, date is seen to have a significant effect ($F(1, 38) = 46.253$, $p < 0.01$), but the effect of shell is clearly stronger ($F(1, 38) = 115.302$, $p < 0.01$) (see Table 10). This is also evident in effect sizes, as the partial Eta Squared for date is 0.562, while the statistic for shell is 0.762. Finally, when we conduct the same one-way ANOVA but include date as a control variable, thereby introducing an ANCOVA, we see that shell has a stronger effect than before ($F(1, 37) = 63.473$, $p < 0.01$) (partial Eta Squared = 0.632) (see Table 11). In addition, these three statistics further support our claim regarding the effect of printed shells, as all three emphasize the substantial difference between natural and printed shells. In summary, it is clear that the effects of the differences in shell type stand even when accounting for possible differences due to the weather. In short, thanks to the actions of the hatchery, we believe we accounted for hurricane activity best as we could. Still, it certainly is possible that the presence of the hurricane affected settlement rates.

Table 9: Post Hoc Analyses. Effect of Shell across July and September

Effect of Shell: ANOVA	Mean Square	F	P
Between Groups	8323.225	37.242	<0.001
Within Groups	223.448		

Table 10: Post Hoc Analyses. Date and Shell			
Effect of Date and Shell: ANOVA	Partial Eta Squared	F	p
Date	0.562	46.253	<0.001
Shell	0.762	115.302	<0.001
Date*Shell	0.416	25.639	<0.001

Table 11: Post Hoc Analyses. Shell with Date as Covariate			
Effect of Date and Shell: ANCOVA	Partial Eta Squared	F	p
Date	0.429	27.764	<0.001
Shell	0.632	63.473	<0.001

Fourier Transform-Infrared Spectroscopy

To better understand our results, we wanted to look into the exact chemical makeup of LAYBRICK. To do this, we planned on using Fourier Transform Infrared Spectroscopy (FTIR). However, since LAYBRICK is copyrighted property, we cannot report on its contents without explicit permission from the creator. None was given, so we could not look into exact numbers on the makeup of the filament.

Future Directions

Further research into this area would provide more insight into the use of printed material in restoration efforts. Of primary interest would be an in-depth study of the components of the LAYBRICK filament. With this knowledge, we would be

able to hypothesize about why spat failed to settle on the printed shells. This detail would also enable future researchers to employ another filament type that could address these concerns. If the spat settled on this substrate, perhaps the door would be opened further for oyster restoration research. This knowledge would further add insight to the idea that chemical composition overrides geometric structure, as the new printouts would be in the shape of a shell with a more suitable chemical composition. In short, this study could eventually be replicated with a filament other than LAYBRICK in effort to see different results.

Future research could also use other methods to produce alternative substrate. For example, researchers could use molding to create shells without using a FDM printer and employing plastics. This might be more suitable because, in theory, we could use calcium carbonate directly to mold a shell into a desirable shape, instead of using a material that has additional compounds in it. Similarly, future research could return to investigating electrolysis. The methodology we applied could be refined such that electrolysis would produce more desirable results. Given that in theory, electrolysis could produce substrate that is primarily calcium carbonate, the process could be crucial in oyster restoration research.

Finally, future research could also investigate using alternative settlement cues, as opposed to L-DOPA. As noted in our study, L-DOPA may decrease the likelihood of oyster settlement in some circumstances. Before deciding on L-DOPA, the team also considered alternatives like GABA. It could be that another chemical cue could produce different results with respect to settlement on the printed material, or alternative substrate generally.

General Conclusion

Eighteen million people live in the watershed of the Chesapeake Bay, and every year, due to the actions of these people, the health of this vital estuary is diminished. The collapsing population size of the eastern oyster is a near perfect representation of that health risk. The eastern oyster is a keystone species, ecosystem engineer, and filter feeder, meaning that its survival is imperative to the continuity of the entire biological community of the Bay. Our overarching goal was to develop and investigate innovative ideas for eastern oyster restoration, in hopes of preserving the Chesapeake Bay.

In the first part of our project, we explored the use of electrolysis mineral accretion to create an artificial reef structure for oyster settlement in the Chesapeake Bay. The limiting factor of oyster population regeneration is insufficient settlement surfaces. By creating a new substrate, with a similar mineral composition to natural shells, we could restore the number of settlement surfaces and restore the oyster population. Inspired by the success of electrolysis to create coral reef structures, we attempted to accrete calcium carbonate onto a rebar structure to construct a proxy oyster reef. Despite attempts in a laboratory setting and flow-through system, an insufficient amount of calcium carbonate accreted onto the structure for settlement testing to proceed. From this process, we learned electrolysis would not be a feasible option for oyster restoration, given the resources we had available.

Motivated by the addition of new team members with 3D printing expertise, our project shifted in a new direction, incorporating additive manufacturing and changing our specific intention. We now wanted to create an oyster shell replica, identical to natural shells in structure, but lacking any biochemical factors. This artificial shell could be used as a blank model in settlement research, helping

biologists determine exactly which environmental cues and physiological factors drive spat settlement. To do this, we used 3D scanning technology to obtain a digital image of the exact 3D structure of numerous natural shells. These scans were then 3D printed using LAYBRICK filament, which contains calcium carbonate. The 3D printed shells were then compared to their natural counterparts for rates of spat settlement. While some spat settled on the 3D printed shells, a significantly larger amount settled on the natural shells. In hopes of spurring more settlement on the artificial shells, we conducted another experiment and added the variable L-DOPA , a chemical stimulant of settlement. Still, the oysters settled more on the natural shells which indicates a multifactorial causation to settlement.

Both of these attempts made a compelling contribution to the field of oyster ecology and Chesapeake Bay restoration. Electrolysis should be further explored to create large-scale oyster reef structures within the Bay. 3D scanning and printing can continue to be used as a system to produce shell replicas for oyster physiology and development research. Overall, more research is needed to find solutions for the collapsing eastern oyster population before the Chesapeake Bay must face the irreparable consequences of extinction.

References

Allen, J., Grady, Q., Koenigsberg, D., McEwen, C., Meredith, M., & St. Clair, J. (2014, December). The Oyster Banks: A Dive into the Political, Scientific, and Social Realms of Oysters and Oyster Aquaculture in North Carolina. University of North Carolina at Chapel Hill, 1-14.

Baker, S. M., & Mann, R. (1994). Description of metamorphic phases in the oyster Crassostrea virginica and effects of hypoxia on metamorphosis. *Marine Ecology Progress Series*, *104*, 91.

Beseres Pollack, J., Yoskowitz, D., Kim, H.-C., & Montagna, P. A. (2013). Role and Value of Nitrogen Regulation Provided by Oysters (Crassostrea virginica) in the Mission-Aransas Estuary, Texas, USA. *PLoS ONE*, *8*(6). https://doi.org/10.1371/journal.pone.0065314.

Burke, R. D. (1983). The induction of metamorphosis of marine invertebrate larvae: stimulus and response. Canadian journal of Zoology, 61(8), 1701-1719.

Byron, C. J., Jin, D., & Dalton, T. M. (2015). An Integrated ecological–economic modeling framework for the sustainable management of oyster farming. Aquaculture, 447, 15–22. https://doi.org/10.1016/j.aquaculture.2014.08.030.

Carroll, J. M., Riddle, K., Woods, K. E., & Finelli, C. M. (2015). Recruitment of the eastern oyster, Crassostrea virginica, in response to settlement cues and predation in North Carolina. Journal of experimental marine biology and ecology, 463, 1-7.

Chesapeake Bay Foundation. (n.d.). What We Have to Lose Economic Importance of the Chesapeake Bay. Retrieved February 19, 2016, from http://www.cbf.org/aboutthebay/issues/costofcleanwater/economicimportanceofthebay.

Correll, D. L. (1998). The role of phosphorus in the eutrophication of receiving waters: A review. Journal of Environmental Quality, 27(2), 261-266.

Dickinson, G. H., Ivanina, A. V., Matoo, O. B., Portner, H. O., Lannig, G., Bock, C., … Sokolova, I. M. (2012). Interactive effects of salinity and elevated CO2 levels on juvenile eastern oysters, Crassostrea virginica. Journal of Experimental Biology, 215(1), 29–43. https://doi.org/10.1242/jeb.061481.

Doney, S. C., Fabry, V. J., Feely, R. A., & Kleypas, J. A. (2009). Ocean Acidification: The Other CO2 Problem. Annual Review of Marine Science, 1, 212-252. doi:10.1146/annurev.marine.010908.163834.

Fertig, B., Carruthers, T. J., & Dennison, W. C. (2014). Oyster δ15N as a Bioindicator of Potential Wastewater and Poultry Farming Impacts and Degraded Water Quality in a Subestuary of Chesapeake Bay. Journal Of Coastal Research, 30(5), 881-892. doi:10.2112/jcoastres-d-11-00231.1.

Gazeau, F., Parker, L. M., Comeau, S., Gattuso, J.P., O'Connor, W. A., Martin, S., Ross, P. M. (2013). Impacts of ocean acidification on marine shelled molluscs. Marine Biology, 160(8), 2207–2245. http://doi.org/10.1007/s00227-013-2219-3.

Goldsborough B., & Pelton, T. (2010, July). On the Brink: Chesapeake's Native Oysters: What it Will Take to Bring Them Back. The Chesapeake Bay Foundation Reports. Retrieved from http://www.cbf.org/document.doc?id=523.

Goreau, T. J. (2012). Electrolysis. In V. Linkov (Ed.), Marine Electrolysis for Building Materials and Environmental Restoration. Rijeka, Croatia: InTech Publishing. https://doi.org/10.5772/48783.

Goreau, T. J., & Trench, R. K. (Eds.). (2013). Innovative methods of marine ecosystem restoration. CRC Press.

Grabowski, J. H., Brumbaugh, R. D., Conrad, R. F., Keeler, A. G., Opaluch, J. J., Peterson, C. H., … Smyth, A. R. (2012). Economic Valuation of Ecosystem Services Provided by Oyster Reefs. Bioscience, 62(10), 900–909.

Hargis, W. J., & Haven, D. S. (1988). The imperilled oyster industry of Virginia: A critical analysis with recommendations for restoration (No. 290). Virginia Sea Grant Marine Advisory Services, Virginia Institute of Marine Science.

Hilbertz, W. (1979). Electrodeposition of minerals in sea water: Experiments and applications. IEEE Journal of Oceanic Engineering, 4(3), 94–113. http://doi.org/10.1109/JOE.1979.1145428.

Hilbertz, W., Fletcher, D., & Krausse, C. (1977). Mineral Accretion Technology: Applications for Architecture and Aquaculture. ResearchGate, 8(4–5). Retrieved from https://www.researchgate.net/profile/Desmond_Fletcher/publication/269096552_Mineral_Accretion_Technology_Applications_for_Architecture_and_Aquaculture/links/547f76200cf250f1edbdc6cd/Mineral-Accretion-Technology-Applications-for-Architecture-and-Aquaculture.pdf.

Hopkins, J. S., Sandifer, P. A., DeVoe, M. R., Holland, A. F., Browdy, C. L., & Stokes, A. D. (1995). Environmental impacts of shrimp farming with special reference to the situation in the continental United States. Estuaries, 18(1), 25–42. https://doi.org/10.2307/1352281.

Horn Point Lab Oyster Hatchery (n.d.). Oyster Life Cycle. Retrieved from http://hatchery.hpl.umces.edu/oysters/oysters-life-cycle/.

Howarth, R. W., & Marino, R. (2006). Nitrogen as the limiting nutrient for eutrophication in coastal marine ecosystems: evolving views over three decades. Limnology and Oceanography, 51(1part2), 364–376.

Kasperski, S., & Wieland, R. (2009). When is it Optimal to Delay Harvesting? The Role of Ecological Services in the Northern Chesapeake Bay Oyster Fishery. Marine Resource Economics, 24(4), 361-385.

Kennedy, V. S., Newell, R. I. E., & Eble, A. F. (1996). The Eastern Oyster: Crassostrea Virginica. Maryland Sea Grant College.

Kerr, S. J. (1995). Silt, turbidity and suspended sediments in the aquatic environment. Ontario Ministry of Natural Resources Technical Report. Retrieved from http://ontarioriversalliance.ca/wp-content/uploads/2014/07/Silt-Turbidity-and-Suspended-Sediments-in-the-Aquatic-Environment-Marked.pdf.

Kickham, Debbi. Tahiti Is A Hot New Travel Trend For 2019. February 12, 2019. Forbes Magazine. https://www.forbes.com/sites/debbikickham/2019/02/12/tahiti-is-a-hot-new-travel-trend-for-2019/#670e18a42230.

Latchere, O., Fievet, J., Lo, C., Schneider, D., Dieu, S., Cabral, P., . . . Saulnier, D. (2016). Effect of electrolysis treatment on the biomineralization capacities of pearl oyster Pinctada margaritifera juveniles. Estuarine, Coastal and Shelf Science,182, 235-242. doi:10.1016/j.ecss.2016.06.014.

Leight, A. K., Slacum, W. H., Wirth, E. F., & Fulton, M. H. (2011). An assessment of benthic condition in several small watersheds of the Chesapeake Bay, USA. Environmental Monitoring and Assessment, 176(1-4), 483–500. https://doi.org/http://dx.doi.org/10.1007/s10661-010-1599-9

Maryland Department of Natural Resources. (2016). Oyster Management Review: 2010-2015. Maryland Department of Natural Resources, Fisheries Service. Retrieved from https://dnr.maryland.gov/fisheries/Documents/FiveYearOysterReport.pdf.

Maryland Department of Natural Resources (n.d.). Sanctuaries. Retrieved from https://dnr.maryland.gov/fisheries/Pages/oysters/sanctuaries.aspx.

Maryland Environmental Trust. (2013). Annual Report Fiscal Year 2013. Retrieved December 6, 2016, from http://dnr.maryland.gov/met/Documents/PDFs/2013annual_report.pdf.

Maryland Sea Grant. (2013). Chesapeake Bay Facts and Figures. Retrieved from http://www.mdsg.umd.edu/topics/ecosystems-restoration/chesapeake-bay-facts-and-figures.

Miller, A. W., Reynolds, A. C., Sobrino, C., & Riedel, G. F. (2009). Shellfish Face Uncertain Future in High CO2 World: Influence of Acidification on Oyster Larvae Calcification and Growth in Estuaries: e5661. PLoS One, 4(5). http://doi.org/http://dx.doi.org/10.1371/journal.pone.0005661.

Müller, J., Bubler, H., Gobner, M., Rettelbach, T., & Duelli, P. (2008). The European spruce bark beetle Ips typographus in a national park: from pest to keystone species. Biodiversity & Conservation, 17(12), 2979–3001. http://doi.org/http://dx.doi.org/10.1007/s10531-008-9409-1.

National Marine Fisheries Service. 2017. Fisheries Economics of the United States, 2015. U.S. Dept. of Commerce, NOAA Tech. Memo. NMFS-F/SPO-170, 247p.

National Oceanic and Atmospheric Administration (2008). NOAA's National Ocean Service Education: Estuaries. Retrieved September 25, 2016, from

http://oceanservice.noaa.gov/education/kits/estuaries/media/supp_estuar09b_eutro.html.

National Oceanic and Atmospheric Administration. Chesapeake Bay Office. Oysters - Fish Facts. www.chesapeakebay.noaa.gov/fish-facts/oysters.

National Oceanic and Atmospheric Administration. (2015). Tred Avon River Oyster Restoration Tributary Plan: A blueprint for sanctuary restoration, draft (United States of America, NOAA Restoration Center, Maryland Department of Natural Resources, U.S. Army Corps of Engineers, Baltimore District, Oyster Recovery Partnership, Chesapeake Bay Office).

Nayar, K. N., Rajapandian, M. E., Gandhi, A. D., & Gopinathan, C. P. (1984). Larval rearing and production of spat of the oyster Crassostrea madrasensis (Preston) in an experimental hatchery. Indian Journal of Fisheries, 31(2), 233-243.

NCDEQ (n.d.). N.C. Oyster Sanctuary Program. Retrieved from http://portal.ncdenr.org/web/mf/habitat/enhancement/oyster-sanctuaries.

Nestlerode, J. A., Luckenbach, M. W., & O'Beirn, F. X. (2007). Settlement and Survival of the Oyster Crassostrea virginica on Created Oyster Reef Habitats in Chesapeake Bay. Restoration Ecology, 15(2), 273–283. https://doi.org/10.1111/j.1526-100X.2007.00210.x

O'Connell, M. T., Franze, C. D., Spalding, E. A., & Poirrier, M. A. (2005). Biological Resources of the Louisiana Coast: Part 2. Coastal Animals and Habitat Associations. Journal of Coastal Research, (44), 146–161.

Office of Environment & Heritage, New South Wales Government (2013). Stormwater. Retrieved from http://www.environment.nsw.gov.au/stormwater/index.html.

Paynter, K. T. (1996). The effects of Perkinsus marinus infection on physiological processes in the eastern oyster, Crassostrea virginica. Journal of Shellfish Research, 15(1), 119-126.

Paynter, K. T., & Burreson, E. M. (1991). Effects of Perkinsus marinus infection in the eastern oyster, Crassostrea virginica: II. Disease development and impact on growth rate at different salinities. J. Shellfish Res, 10(2), 425-431.

Piazza, B. P., Piehler, M. K., Gossman, B. P., La Peyre, M. K., & La Peyre, J. F. (2009). Oyster Recruitment and Growth on an Electrified Artificial Reef Structure in Grand Isle, Louisiana. ResearchGate, 84(1). Retrieved from https://www.researchgate.net/publication/263534591_Oyster_Recruitment_and_Growth_on_an_Electrified_Artificial_Reef_Structure_in_Grand_Isle_Louisiana.

Reitner, J., & Thiel, V. (Eds.). (2011). Encyclopedia of geobiology (pp. 134-135). Dordrecht: Springer.

Rothschild, B. J., Ault, J. S., Goulletquer, P., & Heral, M. (1994). Decline of the Chesapeake Bay oyster population: a century of habitat destruction and overfishing. Marine Ecology Progress Series, 111(1–2), 29–39.

Sabater, M. G., & Yap, H. T. (2004). Long-term effects of induced mineral accretion on growth, survival and corallite properties of Porites cylindrica Dana. Journal of Experimental Marine Biology and Ecology, 311(2), 355–374. http://doi.org/10.1016/j.jembe.2004.05.013.

Schuhmacher, H., & Schillak, L. (1994). Integrated Electrochemical and Biogenic Deposition of Hard Material—A Nature-like Colonization Substrate. Bulletin of Marine Science, 55, 672-679. Retrieved from

http://umd.library.ingentaconnect.com/content/umrsmas/bullmar/1994/00000055/f0020002/art00034.

Sellers, M.A., and J. G. Stanley. 1984. Species profiles: life histories and environmental requirements of coastal fishes and invertebrates. U.S. Fish Wildl. Serv. FWS/OBS-82/11. U.S. Army Corps of Engineers, TR EL-82-4.

Speights, C. J., Silliman, B. R., & McCoy, M. W. (2017). The effects of elevated temperature and dissolved ρCO2 on a marine foundation species. Ecology and evolution, 7(11), 3808-3814.

Styles, R. (2015). Flow and Turbulence over an Oyster Reef. Journal of Coastal Research, 31(4), 978–985.

Talberth, J., Selman, M., Walker, S., & Gray, E. (2015). Pay for Performance: Optimizing public investments in agricultural best management practices in the Chesapeake Bay Watershed. Ecological Economics, (118), 252-261.

Tolley, S. G., & Volety, A. K. (2005). The Role of Oysters in Habitat Use of Oyster Reefs by Resident Fishes and Decapod Crustaceans. Journal of Shellfish Research, 24(4), 1007–1012. https://doi.org/10.2983/0730-8000(2005)24[1007:TROOIH]2.0.CO;2.

Trialfhianty, T. I. (2017). The role of the community in supporting coral reef restoration in Pemuteran, Bali, Indonesia. Journal of Coastal Conservation, 21(6), 873-882.

U.S. Army Corps of Engineers, Baltimore and Norfolk Districts (2012). Chesapeake Bay Oyster Recovery: Native Oyster Restoration Master Plan, Maryland and Virginia. http://www.nab.usace.army.mil/Portals/63/docs/Environmental/Oysters/CB_OysterMasterPlan_Oct2012_FINAL.pdf.

Waldbusser, G. G., Voigt, E. P., Bergschneider, H., Green, M. A., & Newell, R. I. E. (2011). Biocalcification in the Eastern Oyster (Crassostrea virginica) in Relation to Long-term Trends in Chesapeake Bay pH. Estuaries and Coasts, 34(2), 221–231.

Wilber, D. H., & Clarke, D. G. (2001). Biological Effects of Suspended Sediments: A Review of Suspended Sediment Impacts on Fish and Shellfish with Relation to Dredging Activities in Estuaries. North American Journal of Fisheries Management, 21(4), 855–875. https://doi.org/10.1577/1548-8675(2001)021<0855:BEOSSA>2.0.CO;2.

Wilberg, M., Livings, M., Barkman, J., Morris, B., & Robinson, J. (2011). Overfishing, disease, habitat loss, and potential extirpation of oysters in upper Chesapeake Bay. Marine Ecology Progress Series, 436, 131–144. https://doi.org/10.3354/meps09161.

Williamson, T. R., Tilley, D. R., & Campbell, E. (2015). Emergy analysis to evaluate the sustainability of two oyster aquaculture systems in the Chesapeake Bay. Ecological Engineering, 85, 103–120. https://doi.org/10.1016/j.ecoleng.2015.09.052.

Yu, Z., & Guo, X. (2006). Identification and mapping of disease-resistance QTLs in the eastern oyster, Crassostrea virginica Gmelin. Aquaculture, 254(1), 160-170.

Zamani, N. P., Bachtiar, R., Madduppa, H. H., Adi, J. W., Isnul, J., Iqbal, M., & Subhan, B. (2010). Study on Biorock® Technique Using Three Different Anode Materials (Magnesium, Aluminum, and Titanium). Jurnal Ilmu Dan Teknologi Kelautan Tropis, 2(1). Retrieved from http://journal.ipb.ac.id/index.php/jurnalikt/article/view/7858.